NIST Measurement Services:

Gas Flowmeter Calibrations with the 34 L and 677 L *PVTt* Standards

NIST Special Publication 250-63

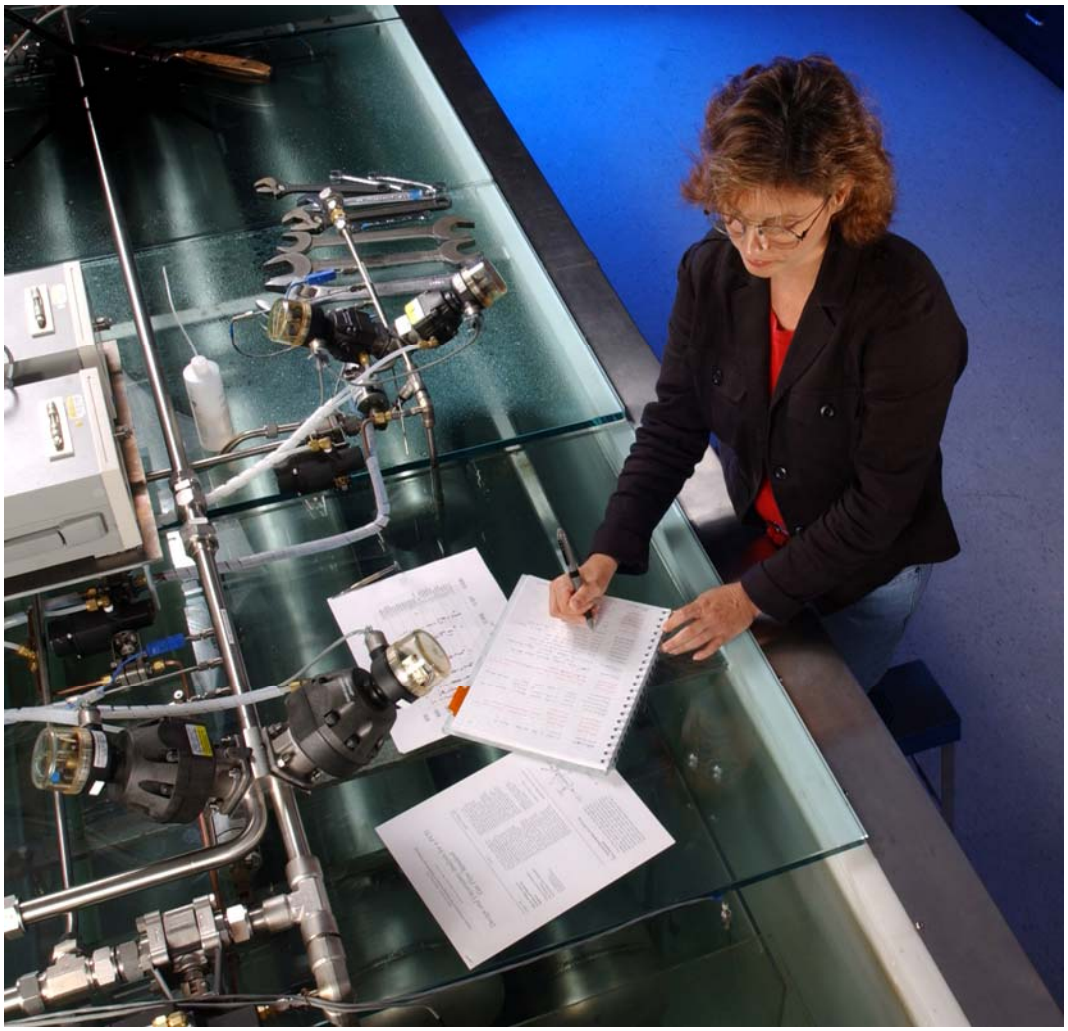

John D. Wright, Aaron N. Johnson, Michael R. Moldover, and Gina M. Kline
November 18, 2010

U. S. Department of Commerce
Technology Administration
National Institute of Standards and Technology

Table of Contents

Abstract

This document provides a description of the 34 L and 677 L pressure, volume, temperature, and time (*PVTt*) primary gas flow standards operated by the National Institute of Standards and Technology (NIST) Fluid Metrology Group. These facilities are used to provide gas flowmeter calibration services as described at the web address: http://ts.nist.gov/MeasurementServices/ for Test Numbers 18010C and 18050C. The *PVTt* standard uses two collection tanks and two diverter valve systems to perform gas flowmeter calibrations between 0.01 L/min and 2000 L/min (the reference temperature and pressure conditions are 293.15 K and 101.325 kPa). The standard measures flow by collecting gas in a tank of known volume during a measured time interval. The uncertainty of the flow measurement is < 0.025 % ($k = 2$ or approximately 95 % confidence level). Over the restricted range from 0.1 L/min to 1000 L/min, the uncertainty was reduced to 0.015 %. The reductions in uncertainty from prior versions of this *PVTt* standard were primarily the result of accurately accounting for the water vapor present in the flowing air. Additional uncertainty reductions result from improved measurements of the pressure and of the collection tank volumes.

We provide an overview of the gas flow calibration service and the procedures for customers to submit their flowmeters to NIST for calibration. We describe the significant and novel features of the standard and analyze its uncertainty. The gas collection tanks have a small diameter and are immersed in a uniform, stable, thermostatted water bath. The collected gas achieves thermal equilibrium rapidly, and the standard uncertainty of the average gas temperature is only 6 mK ($20 \times 10^{-6}\ T$). A novel operating method leads to essentially zero mass change in and very low uncertainty contributions from the inventory volume.

The collection tank volumes were measured gravimetrically, i.e., by transferring a known mass of gas to the evacuated tank and measuring the change in pressure and temperature. Both nitrogen and argon were used. The repeated volume measurements had a standard deviation of $10 \times 10^{-6}\ V_T$ and the standard uncertainty of the volume was $< 58 \times 10^{-6}\ V_T$.

The largest source of uncertainty in the flow measurement can be traced to drift of the pressure sensor calibration over time, which contributes a relative standard uncertainty of 20×10^{-6} to the determinations of the volumes of the collection tanks and to the flow measurements. Throughout the range 3 L/min to 110 L/min, flows were measured independently using the 34 L and the 677 L collection systems, and the two systems agreed within a relative difference of 150×10^{-6}. Double diversions were used to evaluate the 677 L system over a range of 300 L/min to 1600 L/min, and the relative differences between single and double diversions were less than 75×10^{-6}.

Key words: calibration, correlated uncertainty, flow, flowmeter, gas flow standard, inventory volume, *PVTt* standard, mass cancellation, meter, sensor response, uncertainty.

1 Introduction

Calibrations of gas flowmeters are performed with primary standards [1] that are based on measurements of more fundamental quantities, such as length, mass, and time. Primary flow calibrations are accomplished by collecting a measured mass or volume of the flowing fluid over a measured time interval under approximately steady state conditions of flow, pressure, and temperature at the meter under test. The flow measured by the primary standard is computed along with the average of the flow indicated by the meter under test during the collection interval. All of the quantities measured in connection with the calibration standard (i.e., temperature, pressure, time, etc.) are traceable to established national standards. A gas calibration facility consists of a fluid source (e.g., an air compressor or compressed gas cylinders), a test section that provides stable thermodynamic conditions and a fully developed flow profile, and a system for diverting and timing the collection of a quantity of the fluid.

NIST offers calibrations of gas flowmeters in order to provide traceability to flowmeter manufacturers, secondary flow calibration laboratories, and flowmeter users. For a

[1] International Organization for Standardization, *International Vocabulary of Basic and General Terms in Metrology*, 2nd edition, 1993.

calibration fee, NIST calibrates a customer's flowmeter and delivers a calibration report that documents the calibration procedure, the calibration results, and their uncertainty. The flowmeter and its calibration results may be used in different ways by the customer. The flowmeter is often used as a transfer standard to perform a comparison of the customer's primary standards to the NIST primary standards so that the customer can establish traceability, validate their uncertainty analysis, and demonstrate proficiency. Customers with no primary standards use their NIST calibrated flowmeters as working standards or reference standards in their laboratory to calibrate other flowmeters.

Table 1. Primary gas flow calibration capabilities within the NIST Fluid Metrology Group.

Flow Standard	**Flow Range (L/min)**	Gas	**Pressure Range (kPa)**	**Uncertainty (k = 2, %)**
Static Gravimetric	0.001 to 0.1	N_2, Air	100 to 7000	0.05
34 L *PVTt*	0.01 to 100	N_2, Ar, He	100 to 7000	0.025
	0.01 to 100	Air	100 to 1700	0.025
	0.01 to 100	CO_2	100 to 4000	0.025
677 L *PVTt*	10 - 150	N_2	100 to 800	0.025
	10 -2000	Air	100 to 1700	0.025
26 m^3 *PVTt*	860 - 77600	Air	100 to 800	0.09

The Fluid Metrology Group at NIST provides gas flow calibration services over a range of 0.001 L/min to 77 600 L/min.* Table 1 presents the flow ranges covered by the primary gas flow standards in the Fluid Metrology Group. Flows from 900 L/min to 77 600 L/min can be measured with a 26 m^3 *PVTt* standard that was built in the late

* Reference conditions of 293.15 K and 101.325 kPa are used throughout this document for volumetric flows.

1960's and has been upgraded several times [2, 3]. Flows of 0.001 L/min or less can be calibrated by the NIST Pressure and Vacuum Group.

This document describes the theory, methods of operation, and uncertainty of the 34 L and 677 L *PVTt* primary standards that cover the 0.01 L/min to 2000 L/min flow range. From the late 1960's to 2002, this flow range was covered by a set of three mercury-sealed piston provers and two bell provers [4]. The 34 L and 677 L *PVTt* standards were completed in 2002, and for a period of one year we used both the old and the new primary standards for customer calibrations. In 2003, the new primary standards and their uncertainty statements were sufficiently validated [5], and we began using the new standards alone to calibrate customers' flowmeters. An uncertainty analysis for the *PVTt* standards varied between 0.025 % and 0.05 % depending upon what gas a flow range was in use. [6]

In subsequent years, several improvements to the 34 L and 677 L *PVTt* standards were made including, 1) new pressure instrumentation, 2) the addition of a hygrometer to measure the dew point temperature of the air, 3) the direct usage of the NIST properties database (Refprop) [7], and 4) re-determination of the collection tank volumes. These

---

[2] Olsen, L. and Baumgarten, G., *Gas Flow Measurement by Collection Time and Density in a Constant Volume*, Flow: Its Measurement and Control in Science and Industry, ISA, pp. 1287 – 1295, 1971.

[3] Johnson, A. N. and Wright, J. D., *Gas Flowmeter Calibrations with the 26 m^3 PVTt Standard*, NIST Special Publication 250-1046, National Institute of Standards and Technology, Gaithersburg, MD, November 25, 2009.

[4] Wright, J. D. and Mattingly, G. E., *NIST Calibration Services for Gas Flow Meters: Piston Prover and Bell Prover Gas Flow Facilities*, NIST Special Publication 250-49, National Institute of Standards and Technology, Gaithersburg, Maryland, August, 1998.

[5] Wright, J. D., *Gas Flow Measurements and Standards: Development and Validation of a PVTt Primary Gas Flow Standard*, Doctoral thesis to Kogakuin University, Tokyo, Japan, September, 2003.

[6] Wright, J. D., Johnson, A. N., and Moldover, M. R., *Design and Uncertainty Analysis for a PVTt Gas Flow Standard*, J. Res. Natl. Inst. Stand. Technol., **108**, 21–47, 2003.

[7] Lemmon, E. W., McLinden, M. O., and Huber, M. L., *Refprop 23: Reference Fluid Thermodynamic and Transport Properties*, NIST Standard Reference Database 23, Version 9, National Institute of Standards and Technology, Boulder, Colorado, November, 2010.

changes and the resulting uncertainty reductions were documented in a publication [8]. This SP 250 Supplement was updated in November, 2010 to reflect the most recent improvements and uncertainty analysis.

The *PVTt* standard is ideally suited for the calibration of critical flow venturis (CFV's) since they provide pressure isolation and provide a well defined boundary for the inventory volume. A set of NIST CFV's, calibrated by the *PVTt* standards are used as working standards in another calibration facility called the Working Gas Flow Standard (WGFS). The WGFS provides calibrations, particularly for laminar flowmeters, in which the reference flow is measured with uncertainty of 0.1% or less. The methods and uncertainty analysis for the WGFS are covered in a separate document [9].

2 Description of Measurement Services

Customers should consult the web address http://ts.nist.gov/MeasurementServices/Calibrations/mechanical_index.cfm to find the most current information regarding our calibration services, calibration fees, technical contacts, and flowmeter submittal procedures.

NIST uses the *PVTt* primary standards described herein to provide gas flowmeter calibrations for flows between 0.01 L/min and 2000 L/min. The facility has been used at flows as low as 0.005 L/min, but calibrations below 1 L/min should be discussed with the technical contacts before a flowmeter is submitted for such low flows.

The gases available for calibrations in the 34 L *PVTt* standard are dry air, nitrogen, carbon dioxide, argon, and helium. The source of air, at pressures up to 1700 kPa, is an

---

[8] Wright, J. D. and Johnson, A. N., *Lower Uncertainty (0.015 % to 0.025 %) of NIST's Standards for Gas Flow from 0.01 to 2000 Standard Liters / Minute,* Proc. of the 2009 Measurement Science Conference, Anaheim, CA, 2009.

[9] Wright, J. D., Kayl, J.-P., Johnson, A. N., and Kline, G. M., *Gas Flowmeter Calibrations with the Working Gas Flow Standard*, NIST Special Publication 250-80, National Institute of Standards and Technology, Gaithersburg, MD, November 23, 2009.

oil-free reciprocating compressor and a refrigeration drier. The dew point temperature of the dried air is 256 K so the mole fraction of water in the air is 0.13 %. Nitrogen (at pressures up to 800 kPa and purity of 99.998%) is supplied by liquid nitrogen dewars. Higher pressures of nitrogen as well as argon, carbon dioxide, and helium gas can be supplied from compressed gas cylinders. Other non-toxic, non-corrosive gases can be accommodated upon customer request. While other gases are certainly feasible in the 677 L *PVTt* standard, gases are practically limited to air from the compressor and nitrogen from dewars since a very large number of gas cylinders would be necessary to provide gas at 2000 L/min. The gas temperatures are nominally room temperature.

Readily available fittings for the installation of flowmeters in the 34 L and 677 L *PVTt* standards are Swagelok* (1/8" to 1"), A/N 37 degree flare (1/4" to 1"), national pipe thread or NPT (1/8" to 3"), VCR (1/4" and 1/2"), and VCO (1/2" and 1").

Meters can be tested if the flow range, gas, and piping connections are suitable, and if the system to be tested has precision appropriate for calibration with the NIST flow measurement uncertainty. The vast majority of flowmeters calibrated in the gas flow calibration service are either critical flow venturis (critical nozzles) or laminar flowmeters since these are presently regarded as the best candidates for transfer and working standards by the gas flow metrology community [10]. Other meter types that we have tested include positive displacement meters, roots meters, rotary gas meters, thermal mass flowmeters, and turbine meters. Meter types with calibration instability significantly larger than the primary standard uncertainty should not be calibrated with the NIST standards for economic reasons. For example, a rotameter for which the float position is read by the operator's eye normally cannot be read with precison any better than 1 %. It is not practical to pay thousands of dollars to obtain < 0.05 % uncertainty flow data from

---

* Certain commercial equipment, instruments, or materials are identified in this paper to foster understanding. Such identification does not imply recommendation or endorsement by the National Institute of Standards and Technology, nor does it imply that the materials or equipment identified are necessarily the best available for the purpose.

NIST for such a flowmeter when 0.5% data is perfectly adequate and available from other laboratories at significantly lower cost.

A normal flow calibration performed by the NIST Fluid Metrology Group consists of five flows spread over the range of the flowmeter. For a CFV, typical calibration set points are at 200 kPa, 300 kPa, 400 kPa, 500 kPa, and 600 kPa. A laminar flowmeter is normally calibrated at 10 %, 25 %, 50 %, 75 %, and 100 % of the meter full scale. At each of these flow set points, three (or more) flow measurements are made with the *PVTt* standard. The same set point flows are tested on a second occasion, but the flows are tested in decreasing order instead of the increasing order of the first set. Therefore, the final data set consists of six (or more) primary flow measurements made at five flow set points, i.e., 30 individual flow measurements. The sets of three measurements can be used to assess repeatability, while the sets of six can be used to assess reproducibility. For further explanation, see the sample calibration report that is included in this document as an appendix. Variations on the number of flow set points, spacing of the set points, and the number of repeated measurements can be discussed with the NIST technical contacts. However, for data quality assurance reasons, we rarely will conduct calibrations involving fewer than three flow set points and two sets of three flow measurements at each set point.

The Fluid Metrology Group prefers to present flowmeter calibration results in a dimensionless format that takes into account the physical model for the flowmeter type [11]. The dimensionless approach facilitates accurate flow measurements by the flowmeter user even when the conditions of usage (gas type, temperature, pressure) differ from the conditions during calibration. Hence for a CFV calibration, the calibration report will present Reynolds number and discharge coefficient and for a laminar flowmeter, a report presents the viscosity coefficient and the flow coefficient. In order to calculate the

---

[10] Wright, J. D., *What Is the "Best" Transfer Standard for Gas Flow?"*, FLOMEKO, Groningen, the Netherlands, May, 2003.
[11] Wright, J. D., *The Long Term Calibration Stability of Critical Flow Nozzles and Laminar Flowmeters*, National Conference of Standards Laboratories Conference Proceedings, Albuquerque, NM, USA, pp. 443-462, 1998.

uncertainty of these flowmeter calibration factors, we must know the uncertainty of the standard flow measurement as well as the uncertainty of the instrumentation associated with the meter under test (normally absolute pressure, differential pressure, and temperature instrumentation). We prefer to connect our own instrumentation (temperature, pressure, etc.) to the meter under test since they have established uncertainty values based on calibration records that we would not have for the customer's instrumentation. In some cases, it is impractical to install our own instrumentation on the meter under test and the meter under test outputs flow. In these cases, we provide a table of flow indicated by the meter under test, flow measured by the NIST standard, and the uncertainty of the NIST flow value.

3 Pressure, Volume, Temperature, and time (*PVTt*) Standards

PVTt systems have been used as primary gas flow standards by NIST and other laboratories for more than 30 years [2,12,13]. The *PVTt* systems at NIST consist of a flow source, valves for diverting the flow, a collection tank, a vacuum pump, pressure and temperature sensors, and a critical flow venturi (CFV) which isolates the meter under test from the pressure variations in the downstream piping and tank (see Fig. 1).

[12] Kegel, T., *Uncertainty Analysis of a Volumetric Primary Standard for Compressible Flow Measurement*, 3rd International Symposium of Fluid Flow Measurement, San Antonio, TX, USA, 1995.

[13] Ishibashi, M., Takamoto, M., and Watanabe, N., *New System for the Pressurized Gas Flow Standard in Japan*, Proceedings of International Symposium on Fluid Flow Measurements, American Gas Association, 1985.

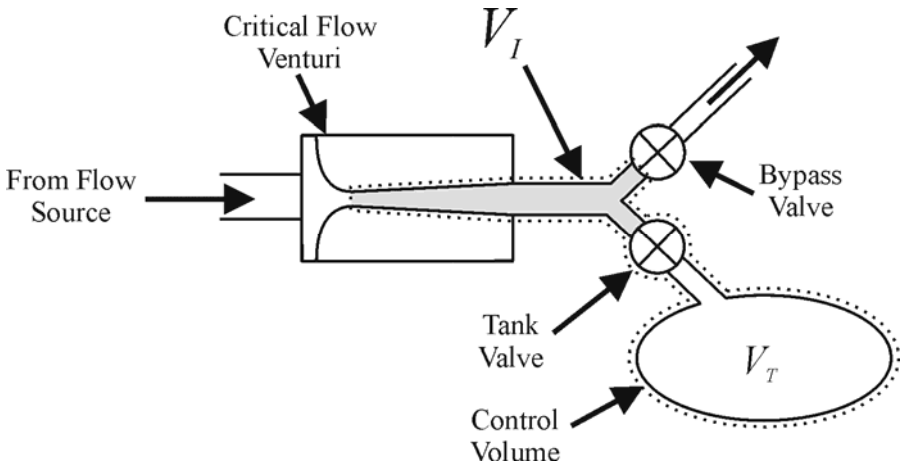

Figure 1. Arrangement of equipment in a *PVTt* system.

The process of making a *PVTt* flow measurement normally entails the following steps:

1. Close the tank valve, open the bypass valve, and establish a stable flow through the CFV.
2. Evacuate the collection tank volume (V_T) with the vacuum pump.
3. Wait for pressure and temperature conditions in the tank to stabilize and then acquire initial values for the tank (P_T^{i} and T_T^{i}). These values will be used to calculate the initial density and the initial mass of gas in the tank (m_T^{i}).
4. Close the bypass valve and, during the "dead-end time" when both the bypass and tank valves are fully closed, choose a start time (t^{i}). At the same time, acquire the initial pressure and temperature in the inventory volume (P_I^{i} and T_I^{i}). These values will be used along with the equation of state for the gas and the inventory volume (V_I) to obtain an initial mass in the inventory volume (m_I^{i}). Shortly after the bypass valve is fully closed, open the tank valve.
5. Wait for the tank to fill to a prescribed upper pressure and then close the tank valve and choose the stop time (t^{f}) during the dead-end time. At the same time, acquire the pressure and temperature in the inventory volume (P_I^{f} and T_I^{f}) and hence the final mass in the inventory. Open the bypass valve.

6. Wait for stability and then acquire P_T^{f} and T_T^{f} and hence m_T^{f}.

By writing a mass balance for the control volume composed of the inventory and tank volumes (see the volume defined by the dashed line in Fig. 1), one can derive an equation for the average mass flow during the collection time:

$$\dot{m} = \frac{(m_T^{\mathrm{f}} - m_T^{\mathrm{i}}) + (m_I^{\mathrm{f}} - m_I^{\mathrm{i}})}{t^{\mathrm{f}} - t^{\mathrm{i}}}, \tag{1}$$

or, neglecting the volume changes between the initial and final conditions:

$$\dot{m} = \frac{V_T\left(\rho_T^{\mathrm{f}} - \rho_T^{\mathrm{i}}\right) + V_I\left(\rho_I^{\mathrm{f}} - \rho_I^{\mathrm{i}}\right)}{t^{\mathrm{f}} - t^{\mathrm{i}}}, \tag{2}$$

where ρ is the gas density determined via a real gas equation of state and pressure and temperature measurements of the gas.

The start and stop times can be chosen at any point during the dead-end time as long as the inventory conditions are measured coincidentally. Why is this true? Implicit in the *PVTt* basis equation (Eq. 2) are two requirements: 1) the measurement of the initial and final densities must be coincident with the measurement of the start and stop times and 2) there must not be any other sources or sinks of mass flow to the control volume. The second condition is met for the entire time that the bypass valve is fully closed, including the start and stop dead-end times. It is not necessary that the initial and final determinations of the mass in the collection tank be done coincidentally with the start and stop times because the tank is free of leaks and it is advantageous to measure these mass values when the tank conditions have reached equilibrium. The freedom to choose the start and stop times from within the dead-end time intervals allows one to choose times where the initial and final inventory densities match, giving essentially zero mass change

in the inventory volume (Δm_I) and extremely good cancellation of certain correlated inventory uncertainties.

The *PVTt* measurement process can be performed in a "blow down" mode also, where initial and final values of the mass in a tank that is the *source* of flow instead of the collector of flow are utilized. Such a system has the advantage that a small compressor can be used to charge a large pressure vessel over a long period of time allowing one to achieve very large flows relatively inexpensively. The blow down method has the disadvantage that it is more difficult to maintain stable pressure and temperature conditions at the meter under test since the high-side pressure of the flow control throttling process is changing continuously as the tank discharges.

The bypass and tank valves can be operated with valve overlap, i.e. where one valve begins to open before the other is fully closed, or with zero overlap, where one is completely closed before the other begins to open (as described above) [14]. With zero overlap, there is no question about lost or extra mass occurring during the diversion. For instance, if the tank is at an initial pressure less than atmospheric, when both valves are partially open, flow can enter the tank from the room instead of through the meter under test. Zero overlap avoids this possibility. For a zero overlap system it is important that any valve design be fast acting. There is a short period of time during the actuation of the diverter valves during which both valves are closed (the "dead-end" time) and the mass of gas that passed through the critical venturi accumulates in the inventory volume. The mass accumulation leads to a pressure rise in the inventory volume that will depend on the mass flow, the size of the inventory volume, and the dead-end time of the diverter valves. The pressure in the inventory must not be permitted to reach a high enough level that the flow at the venturi is no longer critical, lest pressure perturbations reach the meter under test and disrupt the steady state flow conditions at the meter.

[14] Harris, R. E. and Johnson, J. E., *Primary Calibration of Gas Flows with a Weight / Time Method*, Proceedings 2nd International Symposium on Fluid Flow Measurement, Calgary, Canada, pp. 347–358, June, 1990.

4 Design and Operation of the *PVTt* Standard

Experience with a previous, 26 m^3 *PVTt* flow standard at NIST indicated that improvements in temperature and pressure instrumentation as well as in the design and operation of the new system would be necessary in order to achieve an uncertainty of 0.05 % or better [15]. In the following three sections we will describe aspects of the design and operation of the new flow standard that are important to achieve this low uncertainty. The first of these sections describes the measurement of the average temperature of the collected gas. A subsequent section describes the procedures that minimize the uncertainty of the mass change in the inventory volume, and the last section describes the determination of the tank and inventory volumes.

4.1 Average Temperature of the Collected Gas

One of the most important sources of uncertainty in a *PVTt* flow standard is the measurement of the average temperature of the gas in the collection tank, particularly after filling. The evacuation and filling processes lead to cooling and heating of the gas within the volume due to flow work and kinetic energy phenomena [16]. The magnitude of the effect depends on the flow; however, the temperature rise in an adiabatic tank can be 10 K or more. Hence, immediately after filling and evacuation, significant thermal gradients exist within the collected gas. For a large tank, the equilibration time for the gas temperature can be many hours. If the exterior of the tank has non-isothermal or time varying temperature conditions, stratification and non-uniform gas temperatures will persist even after many hours [15].

---

[15] Johnson, A. N., Wright, J. D., Moldover, M. R., and Espina, P. I., *Temperature Characterization in the Collection Tank of the NIST 26 m3 PVTt Gas Flow Standard*, Metrologia, 40, 211–216, 2003.

[16] Wright, J. D. and Johnson, A. N., *Uncertainty in Primary Gas Flow Standards Due to Flow Work Phenomena*, FLOMEKO, Salvador, Brazil 2000.

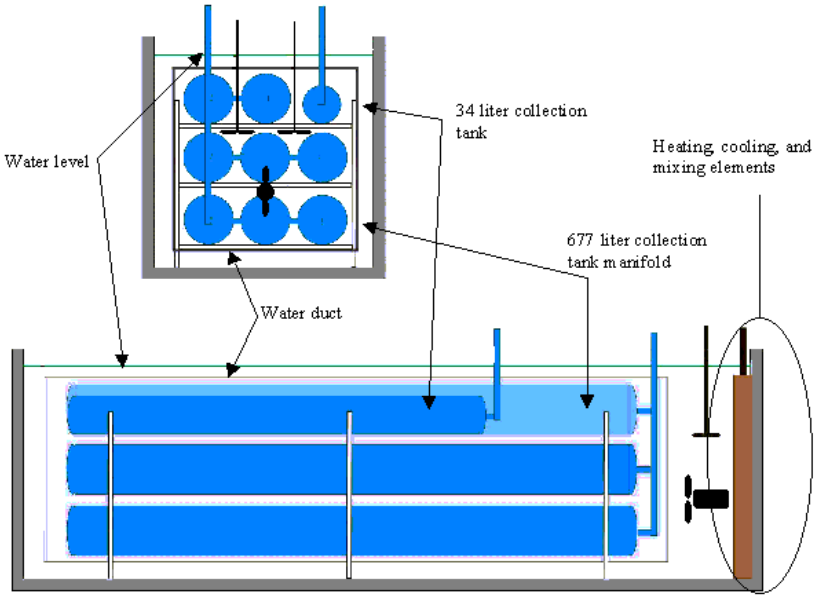

Figure 2. A schematic of the *PVTt* collection tanks, water bath, duct, and temperature control elements.

In this work, we avoided long equilibration times and the difficult problem of measuring the average temperature of a non-uniform gas by designing the collection tanks for rapid equilibration of the collected gas and by immersing the tanks in a well-mixed, thermostatted, water bath (see Fig. 2 and Fig. 3). There are two control volumes, a 34 L collection tank and a 677 L collection tank. Because the equilibration of the 677 L tank is slower, we consider it here. The 677 L tank is composed of eight, cylindrical, 2.5 m long, stainless steel shells connected in parallel by a manifold. Each shell has a wall thickness of $l = 0.6$ cm and an internal radius of $a = 10$ cm. Because all of the collected gas is within 10 cm of a nearly isothermal shell, the gas temperature quickly equilibrates with that of the bath. After the collected gas equilibrates with the bath, the gas temperature is determined by comparatively simple measurements of the temperature of the recirculating water. Remarkably, the water temperature measurements made with 14 sensors had a standard deviation of only 0.4 mK during a typical, 20-minute-long, equilibration interval. In the next section, we describe the bath; in the section after that, we discuss the equilibration of the collected gas.

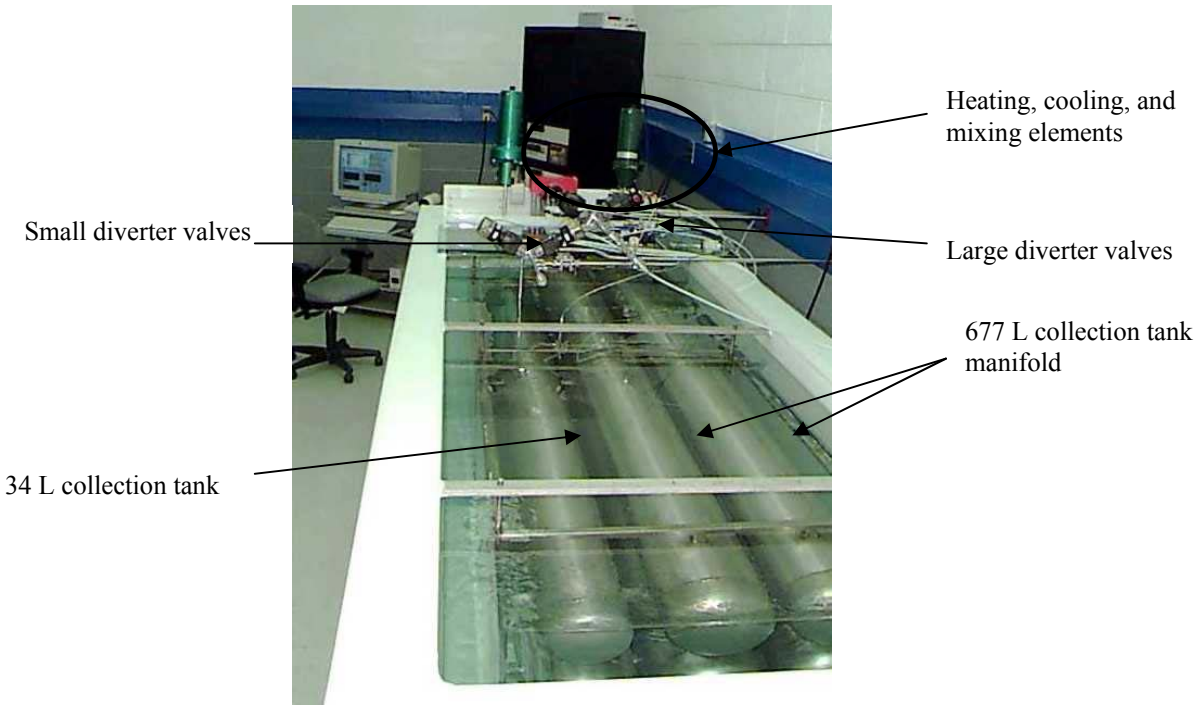

Figure 3. A photograph of the two *PVTt* collection tanks submerged in the temperature controlled water bath.

4.1.1 The Water Bath

The water bath is a rectangular trough 3.3 m long, 1 m wide, and 1 m high. Metal frames immersed in the tank support all the cylindrical shells and a long duct formed by four polycarbonate sheets. The duct surrounds the top, bottom, and sides of the shells: however, both ends of the duct are unobstructed. At the upstream end of the bath, the water is vigorously stirred and its temperature is controlled near the temperature of the room (296.5 K) using controlled electrical heaters and tubing cooled by externally refrigerated, circulated water. A propeller pushes the vigorously stirred water through the duct along the collection tanks. When the flowing water reaches the downstream (unstirred) end of the trough, it flows to the outsides of the duct and returns to the stirred volume through the unobstructed, 10 cm thick, water-filled spaces between the duct and the sides, the top, and the bottom of the rectangular tank.

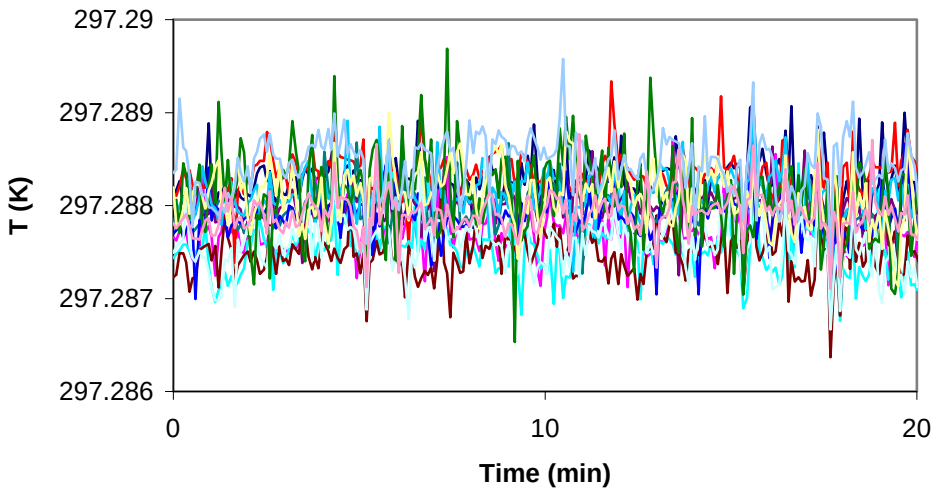

Figure 4. Temperature data for 14 thermistors distributed in the water bath.

The uniformity and stability of the water temperature was studied using 14 thermistors. The thermistors were bundled together and zeroed at one location in the water bath. Then, they were distributed throughout the water bath. Figure 4 plots data recorded at 5 s intervals from these 14 thermistors. Nearly all of the data in Fig. 4 is within ± 1 mK of their mean and the standard deviation of the data from their mean is only 0.4 mK. The largest temperature transients occur where the mixed water enters the duct, indicating incomplete mixing. The tank walls attenuate these thermal transients before reaching the collected gas. Thus, after equilibration, the non-uniformity of the water bath and the fluctuations of the average gas temperature are less than ± 1 mK ($3 \times 10^{-6}\,T$, $k = 1$).

4.1.2 Equilibration of the Collected Gas

For design purposes, we estimated the time constant (τ_{gas}) that characterizes the equilibration of the gas within the collection tank after the filling process. The estimate considers heat conduction in an infinitely long, isotropic, "solid" cylinder of radius a [17]. For the slowest, radially symmetric heat mode, $\tau_{gas} = (a/2.405)^2/D_T$, where D_T is the

[17] Carslaw, H. S. and Jaeger, J. C., Conduction of Heat in Solids, 2nd Edition, Clarendon Press, Oxford, pp 198-201, 1946.

thermal diffusivity of the gas. This estimate gives τ_{gas} = 80 s for nitrogen in the 677 L tank. This estimate for τ_{gas} is too large insofar as it neglects convection, conduction through the ends of the tanks, and the faster thermal modes, all of which hasten equilibration. The time constants for heat to flow from the gas through the tank walls and the time constant for a hot or cold spot within a wall to decay have been calculated and found to be less than a second. Therefore, we expect the collected gas to equilibrate with a time constant of 80 s or less.

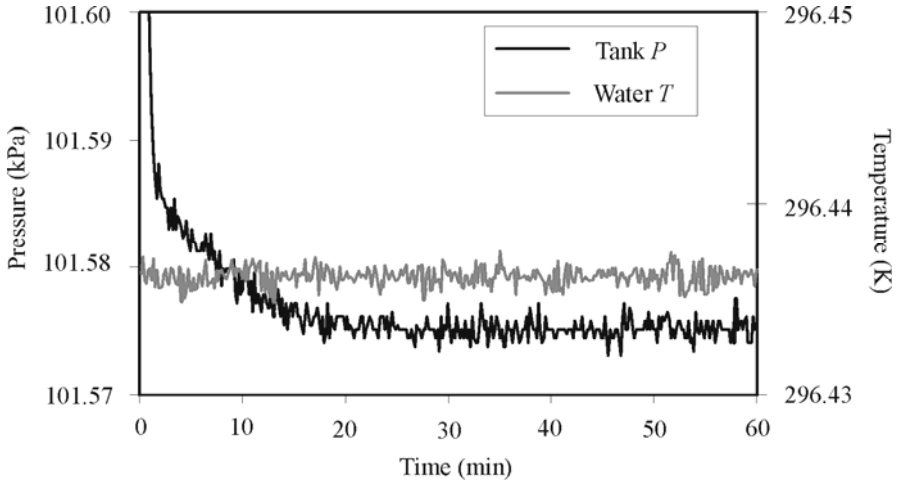

Figure 5. The equilibration of pressure and temperature immediately following a filling of the 34 L tank at 25 L/min.

The equilibration of the collected gas was observed by using the tank as a constant-volume gas thermometer. After the tank valve was closed, the pressure of the collected gas was monitored, as shown in Fig. 5. Our analysis of data such as those in Fig. 5 leads to the experimental values τ_{gas} of less than 60 s for both the 677 L and 34 L tanks, in reasonable agreement with the estimates. The measured time constant and Fig. 5 show that a wait of 20 minutes guarantees that the collected gas is in equilibrium with the bath, within the resolution of the measurements.

The manifold linking the 8 cylindrical shells is completely immersed in the water bath. Thus, the gas in the manifold quickly equilibrates to the bath temperature as well.

However, each collection system has small, unthermostatted, gas filled volumes in the tubes that lead from the collection tanks to the diverter valves, the pressure transducers, etc. In Section 5.4.1, we show the possible temperature variations of these small, unthermostatted volumes make very small contributions to the uncertainty of the gas temperature and the flow measurements.

4.2 Mass Change in the Inventory Volume

4.2.1 Overview and Strategy

As outlined in Section 3, the start time t^i and the stop time t^f used in Eqs. 1 and 2 are chosen to occur during the brief "dead-end times" (< 100 ms) when both the tank valve and the bypass valve are closed, i.e., we use a "zero overlap" diversion [14]. This choice has the advantage of clear mass balance accountability for all the gas flowing through the critical flow venturi during both diversions and the tank filling. Unfortunately, it is difficult to determine either m_I^f or m_I^i and hence the change in mass within the inventory volume accurately (especially at high flows) because both the pressure and the temperature in the inventory volume rise rapidly as the flow through the critical venturi accumulates in the inventory volume (see Fig. 6).

Our strategy for dealing with the inventory mass change has two elements. First, by design, the inventory volume V_I is much smaller than the collection tank volume V_T. (For the 34 L system, $V_T/V_I = 500$; for the 677 L system, $V_T/V_I = 700$.) Thus, the uncertainty of mass flow is relatively insensitive to uncertainty in m_I^f and m_I^i since both are small compared with the total mass of collected gas. Second, we choose t^i near the end of the dead-end time and we chose t^f such that $P(t^i) = P(t^f)$. These choices define a "mass cancellation" method: since the initial and final inventory densities are essentially equal, Δm_I is nearly zero. In fact, we will assume that Δm_I is zero and consider the quantity only in terms of flow measurement uncertainty, not as part of the flow calculation. Symmetry of the inventory transients (see Fig. 7) and the mass cancellation method also give

uncertainty benefits due to high correlation in the uncertainties of pressure and temperature measurements for Δm_I .

We tested our strategy for choosing t^{i} and t^{f} for both the 34 L and the 677 L flow standards. (See Section 6 for details of these tests.) To test the 34 L system, we collected identical flows spanning the range 5 L/min < $\dot{m}$ < 80 L/min in both the small and the large tanks, using the large tank as a reference for the small tank since its inventory uncertainties are quite small in this flow range. To test the 677 L collection system, we collected identical flows in the 677 L tank following two different protocols. In the first protocol, the inventory volume was dead-ended at the beginning and end of the collection interval in the usual manner. In the second protocol the collection interval was divided into two subintervals, which doubled Δm_I and allowed assessment of its uncertainty contribution.

These tests indicate uncertainties due to the inventory volume that are proportional to flow as would be expected based on a thermodynamic model of the inventory pressure and temperature transients. If the inventory uncertainties are considered to arise from uncertainty in the collection time, the inventory mass change uncertainty found experimentally for the 34 L system was $u_{\Delta m_I} = 4 \text{ ms} \times \dot{m}$ (200×10^{-6} $\dot{m}$ for its maximum flow). For the 677 L system, single and double diversions changed the flow measurement by 75×10^{-6} $\dot{m}$ or less.

In the remainder of this section, we describe conditions within the inventory volume during the dead-end times using both a model and measurements. The measurements show that $T(t)$ and $P(t)$ are nearly the same during the start and stop dead-end times. Finally, we show that Δm_I is insensitive to the exact choice of t^{i}, provided that the condition $P(t^{\mathrm{i}}) = P(t^{\mathrm{f}})$ is applied near the end of the dead-end time.

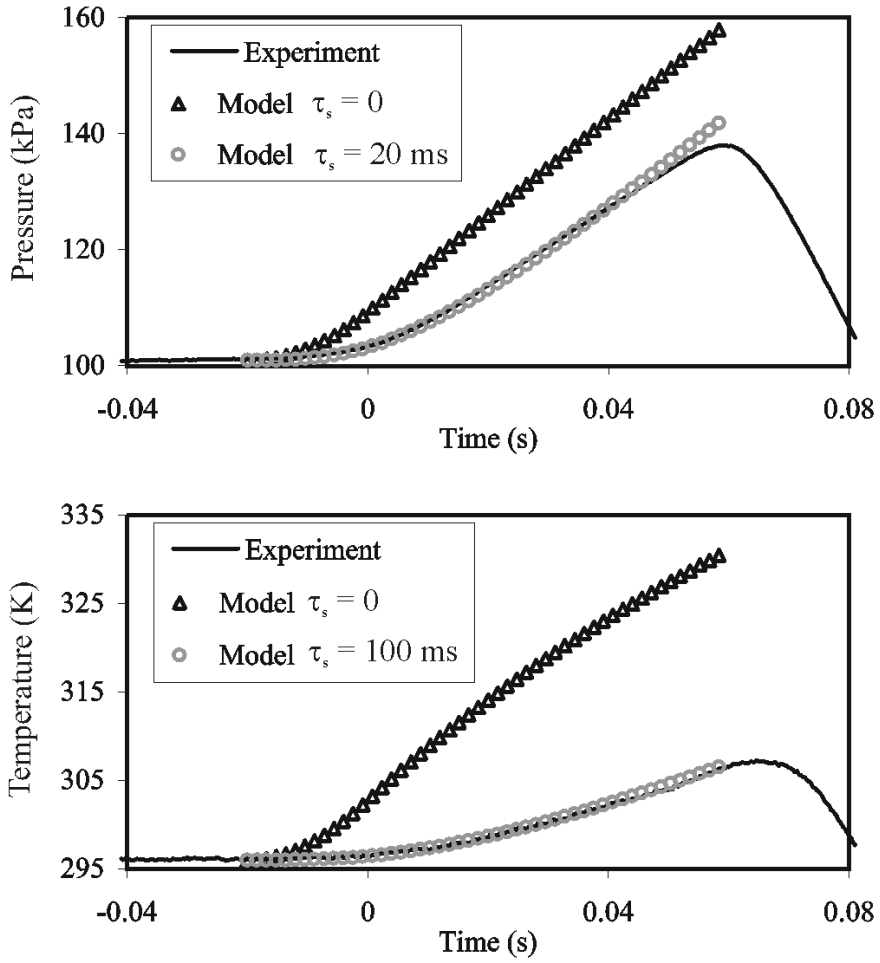

Figure 6. Experimentally measured data (25 L/min in the 34 L tank) and thermodynamic model predictions for zero and non-zero sensor time constants. The model outputs demonstrate that neglect of sensor response causes significant error in the measurement of inventory conditions.

4.2.2 Conditions within the Inventory Volume

Figure 6 displays the time dependent temperature $T(t)$ and pressure $P(t)$ in the inventory volume of the smaller collection system at a typical collection rate ($\dot{m}$ = 25 L/min; collection time = 82 s). The time $t = 0$ in Fig. 6 is defined by the signal indicating that the valve is fully closed. The triangles ($\tau = 0$) in Fig. 6 were calculated from the lumped-parameter, thermodynamic model developed by Wright and Johnson [16]. The model assumes a constant mass flow $\dot{m}$ at the entrance to the inventory volume. The model

neglects heat transport from the gas to the surrounding structure and non-uniform conditions, such as the jet entering the volume. For Fig. 6, $T(t)$ and $P(t)$ were calculated on the assumption that the diverter valve reduced the flow linearly (in time) to zero during the interval $-0.02\ \text{s} < t < 0$. Experimentally measured values of $T(t)$ and $P(t)$ recorded at 3000 Hz (smooth curves) are also shown in Fig. 6. Most of the differences between the measured curve and the ($\tau = 0$) calculated triangles result from the time constants of the sensors used to measure $T(t)$ and $P(t)$. This is demonstrated by the agreement between the experimental curve and the model results when time constants are incorporated (circles).

In Fig. 6, the calculated curves do not display features that mark either the onset or the completion of the diverter valve closing. Thus, even $T(t)$ and $P(t)$ data from perfect sensors cannot be used to mark these events. For this reason, the times t^{i} and t^{f} were chosen at times that were clearly within the dead-end time intervals.

Figure 6 shows that the measured values of $T(t)$ and $P(t)$ are consistent with the Wright-Johnson model for the inventory volume after allowance is made for the response times of the sensors. The consistency shows that the behavior of the inventory volume is understood semi-quantitatively. However, this is not sufficient to accurately calculate the density $\rho(t)$ from measurements of $T(t)$ and $P(t)$ because the fraction of the flow collected as the valves are closing cannot be deduced from the measurements. Instead, we relied on the pressure sensor to choose t^{i}. The pressure sensor is preferred to the temperature sensor because it responds more quickly and also because it responds to the average conditions throughout the inventory volume rather than the conditions at only one location. We choose t^{i} near the end of the dead-end time, where the $P(t)$ measurements are nearly parallel to the $\tau = 0$ model. In this regime, the derivative $\text{d}P/\text{d}t$ is large and its dependence on precisely how the valve closed is small. Because the dependence on how the valve closed has decayed, we expect that $P(t)$ will be the same during the start and the stop dead-end times, improving the mass cancellation as well as the correlation of initial and final inventory density uncertainties.

4.2.3 Near Symmetry of Start and Stop Behavior of *P*(*t*)

Figure 7 shows records of $T(t)$ and $P(t)$ taken during the dead-end time intervals at the start and the stop of a single flow measurement. As before, the data were recorded at 3000 Hz for 500 ms and the plots were displaced along the horizontal axis until they nearly overlapped. The pressure and the temperature at the beginning of the start dead-end time were slightly lower than those at the stop dead-end time; however, the two records match closely during the dead-end time. This implies that the time-dependent densities $\rho(t)$ also nearly match.

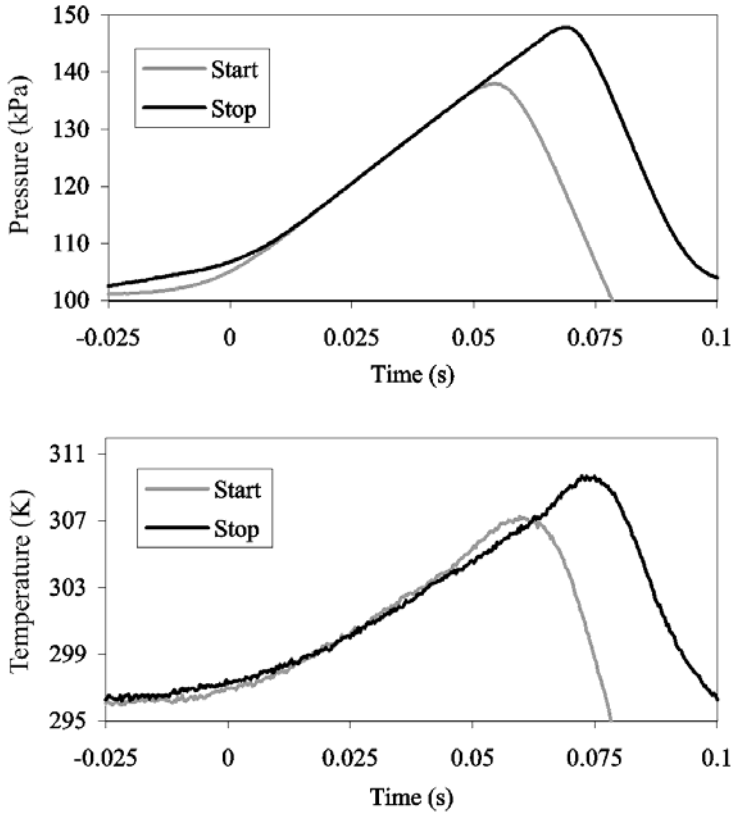

Figure 7. Superimposed inventory data traces for a start diversion and a stop diversion in the 34 L tank at 25 L/min demonstrating "symmetric" diverter valve behavior. The stop dead-end time was approximately 15 ms longer.

At both diversions shown in Fig. 7, valve trigger signals were gathered along with the temperature and pressure measurements using a commercially manufactured data

acquisition card (see Fig. 8). The trigger signals originate from an LED/photodiode pair and a flag on the valve actuator positioned so that the circuit output rises to a positive voltage when the valve is closed. These valve signals are used to trigger timers that give the approximate collection time.

As represented in Fig. 8, the inventory record is post-processed by the controlling program to obtain both the initial and final measurements of pressure and temperature in the inventory volume as well as the final collection time. A "match pressure" $P(t^i)$ is chosen that falls late within the start dead-end interval. The stop time is then found in the stop dead-end interval by choosing $P(t^f) = P(t^i)$. Time corrections between the match pressure measurement and the start and stop trigger signals (Δt^i and Δt^f) are determined from the data record. The appropriate time corrections are added to the approximate collection time from the timers. Thus, by adjusting the collection time using the inventory data records, the initial and final inventory pressures and temperatures are nearly matched, leading to nearly equal initial and final inventory densities and inventory mass cancellation.

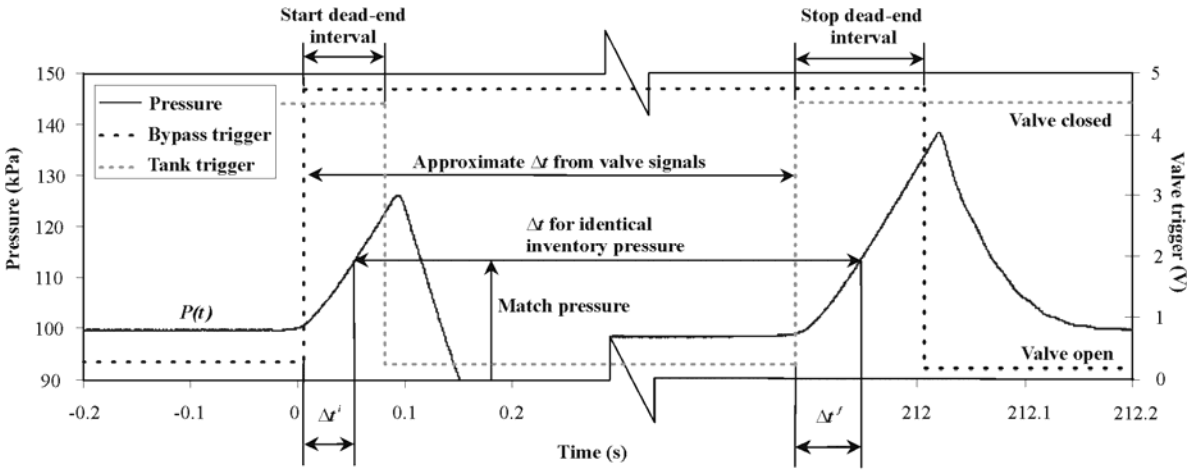

Figure 8. Data records of inventory sensors and valve trigger signals are used to adjust the collection time and improve cancellation of the initial and final inventory mass as well as inventory uncertainties.

4.2.4 Insensitivity of Δm_I to the Match Pressure

Figure 9 shows the total correction time as a function of the match pressure for two flows in the 34 L system. The 100 L/min flow is very high for the 34 L tank, having only an 18 s collection time. Match pressure is shown as a percentage of the range of pressures measured during the diversion transient. For a perfectly fast system (valves and sensors), these plots would be horizontal lines, i.e. any chosen match pressure would result in the same time correction. However, for the real system with its inevitable limitations, the match pressure does matter. Exploring the possible reasons for this is valuable for improving the system and for obtaining an accurate uncertainty analysis.

First recall that the inventory sensors have non-zero time constants and therefore the measurements they provide are damped versions of the real conditions and further, the values they report at any given instant are subject to the recent history of the pressure or temperature value. Second, realize that perfect symmetry of conditions before and during diversion is unobtainable and that these imperfections and the significance of the sensor damping increase with the flow. For example, at high flows, the rate of change of pressure during the tank filling process is large and it becomes more difficult to make the pressure at which the stop diversion begins closely match the pressure at which the start diversion began (due to sensor response and valve control delays). This "trigger pressure difference" will be considered again in Section 6. As another example, the bypass and tank valves may not close at the same speed.

Analysis of the thermodynamic model of the inventory and its sensors shows that times later in the dead-end time give better mass cancellation under these circumstances since the sensor output enters a period with nearly constant slope that is equal to the real pressure slope. The experimental results given in Fig. 9 support this assertion: match pressures between 50 % and 90 % result in nearly constant correction times, while low match pressures (early in the dead-end time) give much larger corrections. Based on this analysis, a match pressure of 80 % has been selected for use in the flow standard. Figure 9 demonstrates the insensitivity of Δm_I to a wide range of match pressure values.

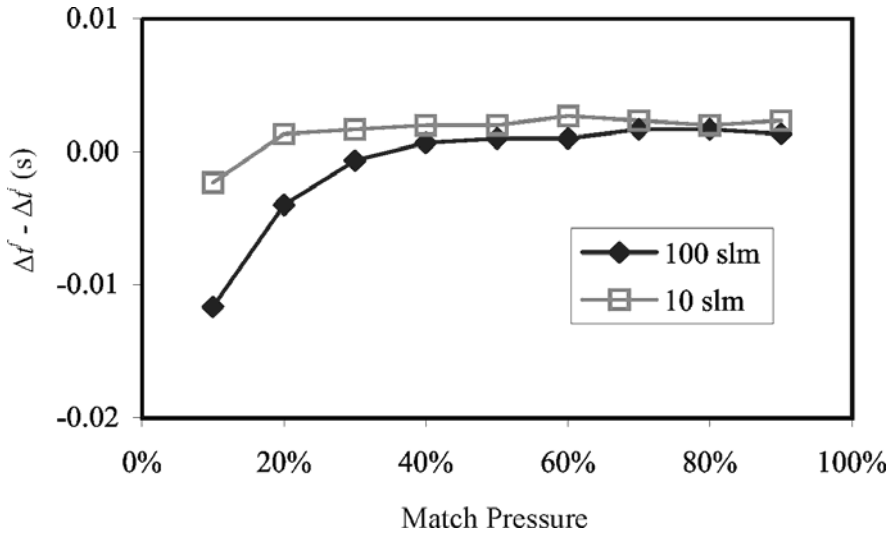

Figure 9. The collection time correction versus the match pressure used in the inventory mass cancellation algorithm.

Figure 9 also illustrates the concept that uncertainties related to the inventory volume can be treated not only as mass measurement uncertainties, but as time measurement uncertainties as well. One can consider the uncertainty in the measurement of time between conditions of perfect mass cancellation, or one can consider the uncertainty in the measurement of inventory mass differences between the start and stop times. Both perspectives offer insight and verification of the uncertainties of the inventory volume and flow diversion process.

4.3 Measurement of the Tank and Inventory Volumes

4.3.1 Gas Gravimetric Method

The volumes of the 34 L and 677 L tanks were determined by the gas gravimetric method. In this method, the mass of an aluminum high pressure cylinder was measured before and after discharging its gas into the evacuated collection tank. The change in mass of the high-pressure cylinder and the change in density of the gas in the collection tank were used to calculate the collection tank volume. Nominally,

$$V_{grav} = \frac{m_c^{\,i} - m_c^{\,f}}{\rho_T^{f} - \rho_T^{i}} - V_{extra}\ , \qquad (3)$$

where the m_c indicates the mass of the high-pressure cylinder and V_{extra} represents the extra volume temporarily connected to the tank for the purpose of introducing the gas from the cylinder to the tank (usually a small volume of tubing and a valve body). The extra volume is calculated from dimensional measurements or measured by liquid volume transfer methods.

In practice, a more complex formula than Eq. 3 was used to account for a small amount of gas that enters the control volume from the room when the cylinder is disconnected from the collection tank since the final tank pressure was less than atmospheric. For the volume determinations performed for the 677 L tank, the effect amounts to only $5 \times 10^{-6}\ V_T$.

The 2002 volume determination was conducted with both nitrogen and argon gas. In both cases high purity gas was used (99.999 %) and care was taken to evacuate and purge the system to minimize composition uncertainties. When nitrogen was used, the aluminum cylinder weighed approximately 4200 g when filled at 12.5 MPa, and approximately 3800 g after it was emptied to 55 kPa. When argon was used, the initial and final masses were 4440 g and 3820 g respectively.

The initial and final masses of the gas cylinder were measured using a substitution process with reference masses and a mass comparator enclosed in a wind screening box. The comparator has a full scale of 10 kg and a resolution of 1 mg. The cylinder and a set of reference masses of nearly the same weight were alternated on the scale 5 times. The zero corrected scale readings were then calibrated to the reference masses and buoyancy corrected via the following formula:

$$m_c = \frac{S_c}{S_{ref}} m_{ref} \left(1 - \frac{\rho_{air}}{\rho_{ref}} \right) + \rho_{air}\ V_{ext}\ , \qquad (4)$$

where *S* represents the scale reading, *ref* indicates the reference masses, ρ_{air} is the ambient air density where the measurements were conducted, and V_{ext} is the external volume of the high pressure cylinder and its valve and fittings. The density of the ambient air was calculated from the barometric pressure, the temperature and humidity inside the wind screen, and an air density formula that includes humidity [18].

The external volume of the high-pressure cylinder appears in Eq. 4 due to air buoyancy corrections. The external volume of the cylinder was measured by Archimedes principle, i.e. by measuring the change in apparent mass of the object in two media with differing and known densities. One of the media was distilled water, and the cylinder apparent mass in the water was measured as follows. Liquid was added to the cylinder interior until it was nearly neutrally buoyant in the tank of distilled water. The addition of liquid inside the cylinder has no effect on its external volume. The temperature of the distilled water was raised or lowered (thereby changing the density of the distilled water) until the cylinder was essentially neutrally buoyant. At this point, the apparent mass in the distilled water is zero. The temperature of the distilled water was recorded and its density was calculated via an equation from the literature [19]. Hence, the temperature of the distilled water was used in place of a weigh scale to measure the apparent mass in water. The apparent mass of the cylinder in air (with the liquid still inside) was measured using the comparator described above. The density of air with humidity was calculated as previously described. The external volume of the cylinder was calculated for the nominal room temperature (T_{ref}) of 296.5 K with the following formula:

$$V_{ext}\left(T_{ref}\right) = \frac{m_{air}^{A} - m_{water}^{A}}{\rho_{water}\left[1 + 3\alpha\left(T_{water} - T_{ref}\right)\right] - \rho_{air}\left[1 + 3\alpha\left(T_{air} - T_{ref}\right)\right]}, \qquad (5)$$

[18] Jaeger, J. B. and Davis, R. S., *A Primer for Mass Metrology*, NBS Special Publication 700-1, National Bureau of Standards, Gaithersburg, Maryland, Eq. 20a, pp. 22, 1984.

[19] Patterson, J. B. and Morris, E. C., *Measurement of Absolute Water Density, 1° C to 40° C*, Metrologia, 31, pp. 277-288, 1994.

where the superscript *A* indicates apparent mass and α is the coefficient of linear thermal expansion for the aluminum tank. The terms containing α correct for changes in the cylinder volume due to differences between the water temperature, the air temperature, and the reference temperature. However, for this particular case, these thermal expansion issues could have been neglected since both the water temperature and air temperature never differed from T_{ref} by more than 1.5 K. The thermal expansion corrections to the external volume were less than 0.5 cm^3 or 100×10^{-6} V_{ext} and the external volume has a small sensitivity coefficient in the collection tank volume determination process.

The expansion of the external cylinder volume as a function of its internal pressure was not negligible. The Archimedes principle measurements showed a volume increase from 4697.5 cm^3 to 4709 cm^3 between the 100 kPa and 12.5 Mpa pressures. This change agreed well with predictions based on material properties, and the appropriate experimental values for external volume were used in the cylinder mass calculations (Eq. 4), depending on whether the cylinder was empty or full. If this issue were neglected, it would lead to relative errors in the mass change measurements of about 35×10^{-6}.

In 2009, a change of pressure and vacuum transducers necessitated re-measuring the collection tank volumes because the network of tubing connecting the sensors to the tanks and the internal volumes of the gauges themselves are part of the collection volume [20]. Re-measuring the volume provided an opportunity for reduction in the *PVTt* uncertainty.

Eight gravimetric measurements of volume were performed on the 677 L tank, two with ultra high purity (UHP) nitrogen (99.999 % N_2) and six with UHP argon. The average of the eight measurements was 677.936 L and the standard deviation of their mean was 10×10^{-6} V_T. Based on the propagation of uncertainty analysis the standard uncertainty for the 677 L volume was reduced from 71×10^{-6} V_T (2002) to 41×10^{-6} V_T (2009), primarily due to improvements in the pressure measurements.

[20] Wright, J. D. and Johnson, A. N., *NIST Lowers Gas Flow Uncertainties to 0.025 % or Less*, NCSL International Measure, **5**, pp. 30 to 39, March, 2010.

As a check, we compared the 2002 measurements of the collection tank volumes to the 2009 volume values. To do so, we measured the volume of the old and new piping and pressure instrumentation networks while they were separated from the collection tanks. These volume measurements were performed for each piping network using the volume expansion method [6] and a reference volume of 0.53775 L. The volume difference between the two piping networks was 0.0485 L. When this difference was applied, the old and new volume measurements for the 677 L tank agreed within $41 \times 10^{-6}\ V_T$, well within our expectations based on the uncertainty analyses.

In 2002, the gravimetric method was used to determine the volume of the 677 L tank and that result was used in a volume expansion method to obtain the 34 L tank volume. The uncertainty for the 34 L tank volume was larger than the 677 L uncertainty ($116 \times 10^{-6}\ V_T$ versus $71 \times 10^{-6}\ V_T$). When the new pressure instruments were installed and the volumes re-measured, the gravimetric method was used for both the 34 L and 677 L volumes. The standard uncertainty in the mass of the pressurized cylinder was 4 mg and this constituted a significant uncertainty for a single filling of the 34 L volume with nitrogen (0.002 g / 38.6 g = 52×10^{-6}). In order to reduce the significance of the mass uncertainty component, the mass change of the cylinder was increased by 1) using a gas with relatively high density (argon), and 2) filling the unknown volume twice and applying the equation:

$$V_{grav} = \frac{m_c^{\mathrm{f}} - m_c^{\mathrm{i}}}{\Delta\rho_1 + \Delta\rho_2} - V_{extra} \qquad (6)$$

where $\Delta\rho = \rho_T^{\mathrm{f}} - \rho_T^{\mathrm{i}}$ and the subscripts 1 and 2 represent the two independent fillings of the unknown volume.

The average of four measurements of the tank volume was 34.0815 L and the standard deviation of their mean was $10 \times 10^{-6}\ V_T$. Using the difference between the old and new

piping networks, the volume measurements for the 34 L tank differed by $29 \times 10^{-6}\ V_T$. The standard uncertainty of the 34 L volume uncertainty was reduced from $116 \times 10^{-6}\ V_T$ to $58 \times 10^{-6}\ V_T$.

5 Uncertainty Analysis of the 34 L and 677 L *PVTt* Flow Standards

In this section, we will analyze the uncertainty of the 34 L and 677 L *PVTt* standards. We will begin by giving an overview of the subject of uncertainty analysis including the issue of correlated uncertainties. Next we will give the results of the uncertainty analysis for mass flow. In following sections, we will give uncertainties of the sub-components that were combined to obtain the mass flow uncertainty.

5.1 Techniques for Uncertainty Analysis

The uncertainty of a mass flow measurement made with the *PVTt* standard use the propagation of uncertainties techniques described in the ISO Guide to the Expression of Uncertainty in Measurement [21]. The process identifies the equations involved in the flow measurement so that the sensitivity of the final result to uncertainties in the input quantities can be evaluated. The uncertainty of each of the input quantities is determined, weighted by its sensitivity, and combined with the other uncertainty components to arrive at a combined uncertainty.

As described in the references [21, 22], consider a process that has an output, y, based on N input quantities, x_i. For the generic basis equation:

$$y = y(x_1, x_2, \ldots, x_N), \tag{7}$$

[21] International Organization for Standardization, *Guide to the Expression of Uncertainty in Measurement*, Switzerland, 1996.

[22] Coleman, H. W. and W. G. Steele, *Experimentation and Uncertainty Analysis for Engineers*, John Wiley and Sons, 2nd edition, 1999.

if all the uncertainty components are uncorrelated, the standard uncertainties are combined by root-sum-square (RSS):

$$u_c(y) = \sqrt{\sum_{i=1}^{N} \left(\frac{\partial y}{\partial x_i} \right)^2 u^2(x_i)}, \tag{8}$$

where $u(x_i)$ is the standard uncertainty for each of the inputs, and $u_c(y)$ is the combined standard uncertainty of the measurand. The partial derivatives in Eq. 8 represent the sensitivity of the measurand to the uncertainty of each input quantity.

In cases where correlated uncertainties are significant (as in the following analysis), the following expression should be used instead of Eq. 8:

$$u_c(y) = \sqrt{\sum_{i=1}^{N} \left(\frac{\partial y}{\partial x_i} \right)^2 u^2(x_i) + 2\sum_{i=1}^{N-1} \sum_{j=i+1}^{N} \frac{\partial y}{\partial x_i} \frac{\partial y}{\partial x_j} u(x_i)\, u(x_j)\, r(x_i, x_j)} \quad , \tag{9}$$

where $r(x_i, x_j)$ is the correlation coefficient, ranging from –1 to 1, and equaling zero if the two components are uncorrelated. As will be seen in the following analysis, some uncertainty components in the present system are correlated and this leads to a significant improvement in the uncertainty of the measurand.

A simple example of a correlated uncertainty is illustrative. Suppose that a thermometer was used to measure a temperature difference. Also suppose that the only uncertainty in the thermometer measurement was an unknown offset in its calibration. When the difference between two temperatures was calculated from measurements made with this thermometer, the offset would cancel and would not contribute to the uncertainty of the temperature difference. In this case, the subtraction process used to calculate the difference leads to sensitivity coefficients of opposite sign for the two temperature measurements. Since the sensor always has the same offset, the uncertainties are perfectly correlated ($r(x_i, x_j) = 1$). When this hypothetical scenario is processed through Eq. 9, the

uncertainty of the temperature difference is zero. Of course in a real case, there would be other, uncorrelated uncertainties that would make the uncertainty of the temperature difference non-zero. Nonetheless, the example demonstrates that under certain circumstances, correlated uncertainties will reduce the uncertainty of a measured quantity.

In the following uncertainty analysis, correlated and uncorrelated uncertainties will be treated as separate components, even if they are related to the same physical quantity. For instance, there will be a correlated as well as an uncorrelated inventory pressure component. In this manner, the correlated components can be considered as having a correlation coefficient of 1, while uncorrelated components have correlation coefficients of 0. This approach simplifies the process to deciding which uncertainty sources are correlated versus uncorrelated and checking that the assumption of perfect correlation is reasonable.

Most of the equations utilized to calculate flow, mass, volume, and other necessary intermediate quantities for the *PVTt* standard have been discussed in prior sections. In Fig. 10 the information is summarized in a diagram that shows the measurement chain used to calculate flow. At the top of the diagram is the output, mass flow. At the second level are the inputs to Eq. 2, the quantities needed to calculate mass flow: density, volumes, and collection time. To calculate density, the inputs to the equation of state are necessary: pressure, temperature, compressibility, the universal gas constant, and molecular mass. The other necessary quantities and their basis equations are shown as well. Figure 10 will serve as a guide for the *PVTt* uncertainty analysis.

The discharge coefficient resulting from a flowmeter calibration will have additional uncertainties not considered herein due to measurements associated with the meter under test. For instance, if the meter under test is a critical flow venturi, uncertainties related to the temperature and pressure measurements at the meter must be included in the uncertainty of the discharge coefficient.

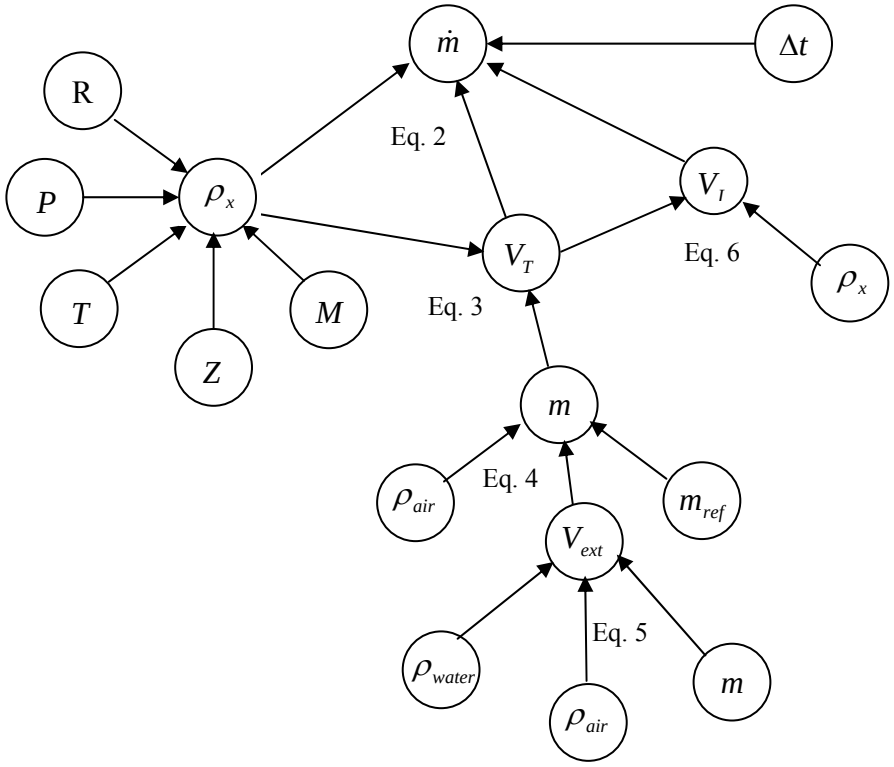

Figure 10. The chain of measurements and equations used for the *PVTt* flow standard.

Unless otherwise stated, uncertainties in this document are $k = 1$, standard, or 68 % confidence level uncertainties. At the conclusion of the uncertainty analysis, a coverage factor of 2 is applied to give an expanded uncertainty for mass flow measurements with an approximate 95 % confidence level. In the remainder of this section, we will give the uncertainty of mass flow for both the 34 L and 677 L *PVTt* systems. In following sections, the uncertainty components that contribute to the *PVTt* mass flow measurement will be traced to their fundamental sources.

5.2 Mass Flow Uncertainty

Table 2 and Table 3 list the major mass flow uncertainty components and their magnitudes for the largest flows calibrated in the 677 L and 34 L *PVTt* standards. The

largest flows are the conditions were the largest mass flow uncertainties occur. Both systems have $k = 2$ uncertainties of approximately 0.025 % or $25 \times 10^{-6}\ \dot{m}$ under worst case conditions.

Table 2. Uncertainty for a 2000 L/min flow measurement with the 677 L standard.

Uncertainty Category	**Standard Uncertainty (k = 1)**		**Contrib**	**Comments**
Flow (677 L, N_2)	**Relative ($\times 10^6$)**		**(%)**	
Tank volume	41	27.48 cm^3	10	see Table 15
Tank initial density	10	1.14×10^{-8} g/cm^3	1	
Tank final density	42	4.21×10^{-8} g/cm^3	11	see Table 9
Inventory mass change	109	0.084 g	74	see Table 21
Collection time	15	0.287 ms	1	see Table 11
Leaks	0	1.3×10^{-7} g/s	0	
Std deviation of repeated meas.	20	0.001 g/s	2	
RSS (combined uncertainty)	**127**			
Expanded uncertainty (k = 2)	**254**			

In Tables 2 and 3, the standard uncertainty of each sub-component is given in both relative ($\times 10^{-6}$) and dimensional forms. The units of the dimensional values are given in the third column. The relative contribution of each sub-component to the combined uncertainty is listed in the fourth column. This contribution is the percentage of the squared individual component relative to the sum of the squares of all sub-components. To calculate their relative uncertainty in the tables, the tank initial density was normalized by the tank final density and the inventory mass change was normalized by the total mass collected.

Table 3. Uncertainty for a 50 L/min flow measurement with the 34 L standard.

Uncertainty Category	**Standard Uncertainty (k = 1)**		**Contrib**	**Comments**
Flow (34 L, N_2)	**Relative ($\times 10^6$)**		**(%)**	
Tank volume	58	1.978 cm^3	27	see Table 16
Tank initial density	10	1.14×10^{-8} g/cm^3	1	
Tank final density	42	4.82×10^{-8} g/cm^3	14	see Table 9
Inventory mass change	82	0.003 g	54	see Table 22
Collection time	7	0.269 ms	0	see Table 11
Leaks	0	1.9×10^{-8} g/s	0	
Std deviation of repeated meas.	20	1.9×10^{-5} g/s	3	
RSS (combined uncertainty)	**112**			
Expanded uncertainty (k = 2)	**224**			

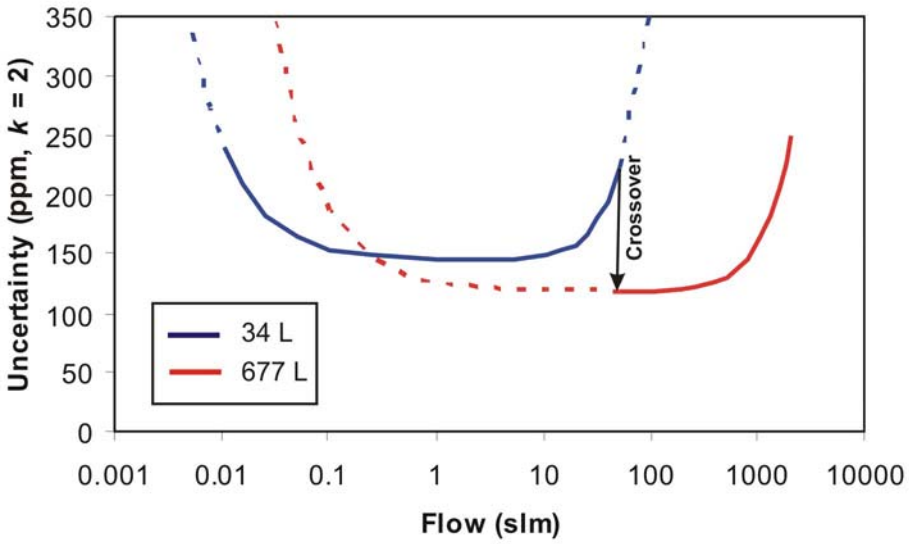

Figure 11. 95 % confidence level (k = 2) *PVTt* uncertainties versus flow in parts per 10^6 (ppm). Dashed lines indicate possible, but normally unused ranges. For both systems, inventory uncertainties dominate at high flows, leaks dominate at low flows, volume and density measurements establish baseline uncertainty in mid-range flows.

Figure 11 presents the results from the propagation of uncertainties model as a function of flow for the 34 L and 677 L flow standards. The high-range end points of the two solid

curves correspond to the uncertainties in Tables 2 and 3. Figure 11 captures two flow dependent components: (1) uncertainties related to the inventory volume and (2) leaks. The flow dependent components cause the uncertainty to increase above baseline levels of approximately 150 ppm at high and low flows. The 150 ppm baseline uncertainty is traceable to the tank volume and final gas density uncertainties (both traceable to pressure). If the crossover flow between the two standards is 50 L/min, the $k = 2$ uncertainty for the mass flow is < 250 ppm from 0.01 L/min to 2000 L/min. Note that the 677 L standard can be used at crossover flows lower than 50 L/min, but the collection times grow inconveniently long.

In the following sections, the uncertainty contributions to mass flow listed in Tables 2 and 3 are decomposed to their detailed sub-components.

5.3 Pressure

A Ruska Model 2465-754 gas lubricated piston pressure gauge is used as the primary pressure standard to calibrate pressure transducers within the Fluid Metrology Group. The uncertainties in a single pressure measurement made with this device are listed in Table 4. Uncertainties in the pressure standard can be traced to the effective area of the piston, piston thermal expansion, the masses, local gravity, and the measurement of the pressure under the bell jar covering the piston and masses (necessary for absolute pressure measurements). The uncertainty shown in Table 4 is for a pressure value of 100 kPa. No buoyancy corrections are made to the masses since the reference pressure, and hence the density under the bell, are small enough that the buoyancy corrections (and uncertainties) are negligible ($<<1 \times 10^{-6} P$). The uncertainty of the piston pressure gauge is $17 \times 10^{-6} P$ at 100 kPa.

Table 4. Uncertainties for a 100 kPa pressure measurement made with the piston pressure gage used as the standard for pressure calibrations.

Uncertainty Category	**Standard Uncertainty (k = 1)**		**Contrib**	**Comments**
	Relative ($\times 10^6$)	**(kPa)**	**(%)**	
Piston Pressure Gage				
Pressure value		100		
piston effective area	12	0.0012	59	from NIST Pressure and Vacuum Group cal.
thermal expansion	6	0.0006	15	assume *T* unc of 0.2 K
masses	1	0.0001	0	Mass Group calibration
local gravity	0.2	0.00002	0	9.801011+/- 0.000002
air density for buoyancy	0	0	0	neg. air density relative to mass density
ref. *P* for absolute	10	0.001	41	based on calibration data of the vac gauge
RSS	**17**	**0.0017**		

5.3.1 Collection Tank Pressure

Measurements of the collection tank initial pressure are made with a pair of MKS Model 626A capacitance diaphragm gauges (CDGs), with full scale of 1300 Pa, that have been calibrated by comparison to a reference vacuum system. Based on the periodic calibration results, the level of agreement between the redundant sensors, and the repeatable readings of the gauges at the vacuum pump ultimate pressure, a standard uncertainty of 1 Pa will be used. As will be seen when the components are combined to give the flow measurement uncertainty, the sensitivity of the flow measurement to this uncertainty component is small due to the low initial pressure in the collection tank (20 Pa).

Pressure measurements of the full collection tank are made with a pair of Yokogawa MT210 resonant silicon pressure gauges with a full scale of 130 kPa. The pressure gauges are periodically calibrated against the piston pressure gauge. The transducer outputs are corrected with a first order equation, i.e. the corrected reading = A0 + A1 ×

reading, and this correction gives residuals with standard deviation of 8×10^{-6} P over the range of pressures of the full tank (40 kPa to 100 kPa). The zero offset and slope from the periodic calibrations of the transducers conducted during 5 years are plotted versus time in Figure 12. The zero offsets of both transducers drift at a rate of approximately 0.025 Pa/day. The initial zero drift rate was more than 0.05 Pa/day. The drift rate of the transducer slope also changed during the 5 years; initially it was 8×10^{-8}/day and now it is essentially zero.

The two transducers behaved in remarkably similar ways. Surely a portion of their correlated behavior can be traced to the fact that they were calibrated in parallel with the same piston pressure gauge. However, the shapes of the curves in Figure 12 result from the transducers themselves and not from the pressure reference; other pressure transducers that were calibrated with the same reference have different aging characteristics.

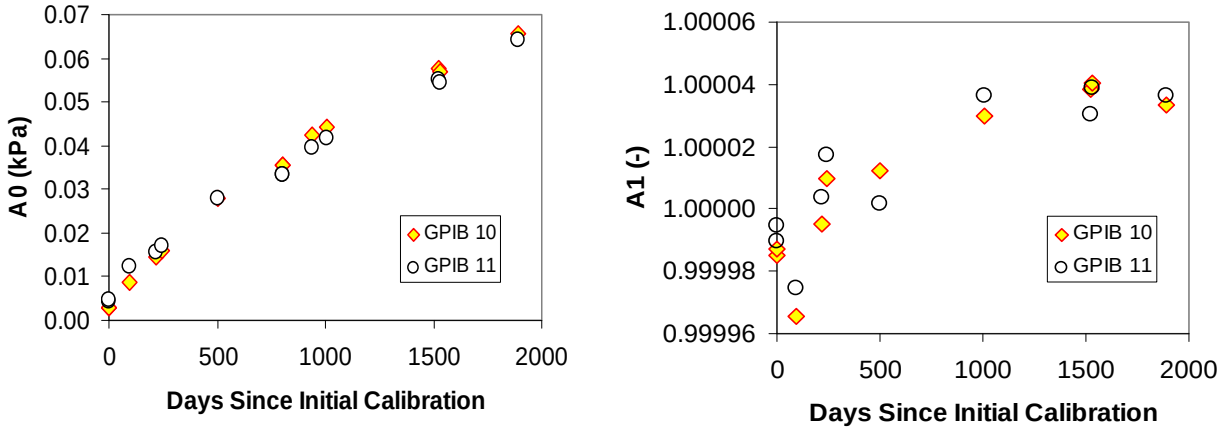

Figure 12. Zero offset (A0) and slope (A1) corrections for the two pressure transducers used to measure full tank pressure as a function of time since their initial pressure calibration performed on July 22, 2003.

The calibration drift of the pressure transducers is sufficiently predictable that one year after a calibration, they will read in error by 0.035 Pa/day × 365 days = 9 Pa or 90×10^{-6} P. In January 2009, we adopted the practice of using the pressure from the CDGs each time the collection tank is evacuated for a new flow measurement to adjust the zero offset

of the pressure transducers. With this approach, uncertainties due to drift in the pressure transducers was reduced to $20 \times 10^{-6} P$. Incorporating uncertainties due to the piston pressure gauge used for pressure calibrations, fit residuals, hysteresis, and thermal effects leads to a full tank pressure uncertainty of $30 \times 10^{-6} P$.

The uncertainties in the collection tank pressure measurement are listed in Table 5. They include the uncertainties from the piston pressure gage, the long term drift of the pressure transducers (quantified by periodic re-calibrations), as well as the residuals from the best fit calibration equation (including hysteresis), and thermal effects. Uncertainties due to spatial non-uniformity of pressure within the tank and time response of the sensor are negligible since the calibration procedure is to wait 10 minutes for equilibration before the measurements are made.

Table 5. Uncertainties in the collection tank pressure measurement at 100 kPa.

Uncertainty Category	**Standard Uncertainty (*k*=1)**		**Contrib**	**Comments**
	Relative (×10^6)	**(kPa)**	**(%)**	
Pressure Measurement				
Pressure value		100		
piston pressure gage	17	0.0017	32	from Table 4
drift	20	0.0020	46	from cal, records
residuals, hysteresis, thermal effects	14	0.0014	22	from cal. records, experiments
RSS	**30**	**0.0030**		

5.4 Temperature

The temperature sensors used in the flow standard are traceable to the NIST Thermometry Group through calibrations made with a four-wire thermister transfer standard (Thermometrics Model TS8901) and a recirculating water constant temperature bath. The uncertainty of the transfer standard thermister is 1 mK (see Table 6). The drift

of the transfer standard is considered negligible based on > 10 annual calibrations that have always differed from each other by less than the calibration uncertainty.

Table 6. Uncertainties for the Fluid Metrology Group temperature transfer standard.

Uncertainty Category	**Standard Uncertainty (k =1)**		**Contrib**	**Comments**
	Relative ($\times 10^6$)	**(mK)**	**(%)**	
Temperature Transfer Standard				
Temperature value		3×10^5		
Thermometry Group cal	3	1	92	unc. for 274 K to 368 K
fit residuals	1	0.3	8	some years, 1/6 this size
drift	0	0	0	less than discernable given cal unc.
radiation, self-heating, etc.	0	0	0	deeply immersed in water bath
RSS	**4**	**1.0**		

5.4.1 Collection Tank Temperature

The measurement of the temperature of the gas in the collection tank has additional uncertainties that are listed and quantified in Table 7. Temperature is measured with YSI Model 46000 thermisters in 3 mm diameter stainless steel sheaths, a Keithley model 224 current source, a Keithley model 7001 switch system, and a Keithley model 2002 multimeter. Uncertainty sources include the temperature transfer standard covered by Table 6, the uniformity and stability of the water bath used to calibrate the thermisters, and the residuals of the best-fit equation to the calibration data. The largest uncertainty component is the calibration drift between periodic calibrations. Radiation and stem conduction are negligible since the thermisters are immersed at least 15 cm in room temperature water. Tests were conducted to measure the significance of self-heating by varying the thermister current while the sensor was held in a stable water bath and watching the resulting change in sensor reading. Based on this experiment, the current through the 5000 ohm thermisters was set to 10 μA which leads to self-heating of less than 1 mK. The *PVTt* bath stability and uniformity (1 mK) were discussed earlier, as was

the issue of thermal equilibrium between the water bath and the gas in the collection tank. The sensors are calibrated over their entire range of usage, so there is no uncertainty related to extrapolation of their calibration data. Uncertainty related to the time response of the thermisters is negligible since the time constant for the sensor is on the order of 10 s and the wait for thermal equilibrium is 30 or more times longer.

Small portions of the gas collection tank are not immersed in the water bath. They include the tubing connecting the outlet of the diverter valve to the collection tank, the tubing that connects the tank to pressure and vacuum transducers, and the internal volume of these transducers. Because we assumed that the bath temperature represents the gas temperature, and the room temperature may differ from that of the bath, the small portion of the tank not immersed leads to a gas temperature uncertainty. The room temperature is maintained at 23.5 ± 1°C. The fractional error in mass contained in the collection tank due to a 1 K difference between the room and the water bath is:

$$\frac{\delta m}{m} \approx \frac{V_{out}}{V_T}\frac{\delta T}{T}, \tag{10}$$

where V_{out} is the volume of the portion of the tank that is at room temperature and δT is the difference between the room and water bath temperatures. For the large tank, V_{out} is 200 cm^3 and the total tank volume is 677 L. For δT of 1 K, the relative mass uncertainty is 1×10^{-6}. This uncertainty will be treated as an uncertainty in the average gas temperature of $1 \times 10^{-6}\ T$ or 0.3 mK in the following analysis. For the small tank this temperature uncertainty is 1.2 mK or $4 \times 10^{-6}\ T$.

By RSS of the components listed in Table 7, the combined uncertainty for the average temperature of the gas in the collection tank is 7 mK when using the thermisters dedicated to the flow standard.

Table 7. Uncertainty of average gas temperature in the collection tank with the dedicated temperature sensors.

Uncertainty Category	**Standard Uncertainty (k =1)**		**Contrib**	**Comments**
	Relative ($\times 10^6$)	**(mK)**	**(%)**	
Tank Gas Average Temperature				
Temperature value		297000		
temperature transfer standard	4	1.0	3	from Table 7
cal. bath uniformity and stability	3	1	3	based on notes made during cal
fit residuals	7	2	12	
drift (I, R, DMM, thermistors)	17	5	72	from cal. records
radiation, stem cond., self-heating	3	1	3	expt. varied current, 5 mK, assume rect.
PVTt bath uniformity and stability	3	1	3	based on experimental measurements
diff. between water and room T's	4	1.2	4	see Eq. 10
extrapolation	0	0	0	cal covers whole operating range
sensor time constant	0	0	0	wait time is >10 × sensor time constant
RSS	**20**	**6**		

5.5 Gas Properties

The NIST gas properties database Refprop [7, 23] is incorporated into Fluid Metrology Group data reduction software via a dynamic link library (dll). Refprop calculates properties (e.g., density, viscosity, and critical flow function) for more than 80 substances as well as for user defined mixtures like moist air. Polynomial fits to Refprop in temperature and pressure had been used since 2003. When a hygrometer was added to the *PVTt* standard in 2008, we began using the Refprop dll instead of the fits to Refprop.

Besides the gas temperature and pressure, contributors to the gas density uncertainty include the gas constant, the molecular mass, and the compressibility. Four gases will be

[23] Available for purchase at http://www.nist.gov/srd/nist23.htm.

considered. Tank volume determinations were conducted with ultra high purity nitrogen (99.999 %) and ultra high purity argon (99.999 %). During normal calibrations, industrial liquid nitrogen vaporized from dewars (99.998 %) and compressed, dried air are used.

5.5.1 Gas Constant

The universal gas constant, $R = 8314.471(m^2\ g)/(s^2\ K\ gmol)$, is known with relative standard uncertainty better than 2×10^{-6} [24].

5.5.2 Compressibility

Uncertainty estimates for experimental studies of compressibility are often unavailable, especially for older publications. Comparison of previously compiled compressibility values obtained by various researchers [25, 26, 27, 28] shows agreement to within 10×10^{-6} in the 270 K to 330 K temperature range at 100 kPa. Perhaps more valuable is that this level of agreement is achieved between compressibility measurements made by the traditional *PVT* method and by the more recent speed of sound techniques [29]. Based on this information, a relative standard uncertainty of 10×10^{-6} will be used for the

---

[24] Moldover, M. R., Trusler, J. P. M., Edwards, T. J., Mehl, J. B., and Davis, R. S., *Measurement of the Universal Gas Constant R Using a Spherical Acoustic Resonator*, NIST J. of Res., 93, (2), 85–143, 1988.

[25] Dymond, J. H. and Smith, E. B., *The Virial Coefficients of Pure Gases and Mixtures: A Critical Compilation*, Clarendon Press, Oxford, 1980.

[26] Hilsenrath, J., Beckett, C. W., Benedict, W. S., Fano, L., Hoge, H. J., Masi, J. F., Nuttall, R. L., Touloukian, Y. S., and Woolley, H. W., *Tables of Thermal Properties of Gases*, NBS Circular 564, 1955.

[27] Lemmon, E. W., Jacobsen, R. T., Penoncello, S. G., and Friend, D. G., *Thermodynamic Properties of Air and Mixtures of Nitrogen, Argon, and Oxygen from 60 to 2000 K at Pressures to 2000 MPa*, J. Phys. Chem. Ref. Data, 29, (3), 331-362, 2000.

[28] Span, R., Lemmon, E.W., Jacobsen, R.T, Wagner, W., and Yokozeki, A. *A Reference Equation of State for the Thermodynamic Properties of Nitrogen for Temperatures from 63.161 to 1000 K and Pressures to 2200 MPa*, J. Phys. Chem. Ref. Data, 29(6):1361-1433, 2000.

[29] Trusler, J. P. M., Wakeham, W. A., and Zarari, M. P., *Model Intermolecular Potentials and Virial Coefficients Determined from the Speed of Sound*, Molecular Physics, 90, (5), pp. 695–703, 1997.

compressibility. This uncertainty is for a pressure of 100 kPa and it scales with density. The uncertainty components of the compressibility factor are listed in Table 8.

Table 8. Uncertainty of the compressibility for nitrogen, argon, and dry air.

Uncertainty Category	**Standard Uncertainty (k =1)**		**Contrib**	**Comments**
Compressibility (Z)	**Relative ($\times 10^6$)**	**(-)**	**(%)**	
Compressibility value		1		
experimental data	10	1×10^{-5}	99	based on analysis of literature
impurity effects on Z	1	1×10^{-6}	1	
residuals of best fit	0	0	0	$<1 \times 10^{-6}$
RSS	**10**	**1×10^{-5}**		

The source of the dry air used in the flow standard is a Joy oil-free two stage reciprocating compressor and a Zurn refrigeration dryer. The mole fraction of water in this air source is 0.0013 ± 0.0005. This uncertainty in composition leads to uncertainty in the compressibility of only 1×10^{-6} Z. The uncertainty in compressibility due to impurities is smaller for the other gases.

5.5.3 Molecular Mass

The departure of the molecular mass of ultra high purity nitrogen, industrial liquid nitrogen, and ultra high purity argon from the molecular mass of the pure substance was examined using the impurity specifications of the gas manufacturer. This analysis results in molecular mass relative standard uncertainties less than 1×10^{-6}, but 1×10^{-6} will be assumed for the molecular mass of nitrogen (28.01348 g/mol) and argon (39.94800 g/mole).

In 2008, an RH Systems model 973 chilled mirror hygrometer with a range of -50 °C frost point to 20 °C dew point temperature was added to the *PVTt* instrumentation. The manufacturer's uncertainty specification is 0.2 °C at the 95 % confidence level;

however, we do not have our own calibration history yet. Therefore, we conservatively assume that the dew point temperature is measured within 0.4 °C with a 95 % confidence level. Since installing the hygrometer, we have observed dew point temperatures as high as -15 °C from our compressor. For this worst case, an uncertainty in the dew point temperature of 0.4 °C results in a 12×10^{-6} fractional uncertainty ($k = 1$) in the molecular mass of the air. In calculating this uncertainty, we account for the relatively small uncertainty contributions (*i.e.*, less than 10 %) from the enhancement factor, the Hyland-Wexler equation used for determining the saturation pressure as a function of the dew point [30, 31], and the pressure head at the chilled mirror.

The uncertainty of the molecular mass of moist air includes two additional contributions, one from the uncertainty of the molecular mass of dry air at fixed CO_2 concentration (see Table 9), and another from the variable amount of CO_2 in the air. The standard uncertainty of the molecular mass of dry air was determined by Picard to be 16×10^{-6} $\mathcal{M}$ [32]. The mole fraction of CO_2 has a nominal value of 385×10^{-6} [33] and is herein assumed to have a standard uncertainty of 13×10^{-6}. The 13×10^{-6} uncertainty accounts for differences in the mole fraction of CO_2 reported by different researchers as well as spatial and temporal variations in CO_2 levels. The uncertainty in the molecular mass of the air resulting from the uncertainty in CO_2 levels is $5 \times 10^{-6} \mathcal{M}$. Combining the uncertainties attributed to water vapor ($12 \times 10^{-6} \mathcal{M}$), the molecular mass of dry air (16×10^{-6} $\mathcal{M}$), and variations in the mole fraction of CO_2 (5×10^{-6}) by root-sum-square (RSS) leads to an air molecular mass uncertainty of 20×10^{-6} $\mathcal{M}$.

---

[30] Hyland, R. W., and Wexler, A., *Formulations for the thermodynamic properties of the saturated phases of H_2O from 173.15K to 473.15 K*, ASHRAE Trans. **89** part IIA, pp. 500–519, 1983.

[31] Hyland R. W. and Wexler, A., *Formulations for the thermodynamic properties of dry air from 173.15K to 473.15 K, and of saturated moist air from 173.15K to 372.15 K, at pressures to 5MPa*, ASHRAE Trans. **89,** part IIA, pp. 520–535, 1983.

[32] Picard, A, Davis, R. S., and Fujii, K., *Revised formula for the density of moist air (CIPM-2007),* Metrologia **45**, pp. 149–155, 2008.

[33] Keeling C. D., Whorf, T.P., and the Carbon Dioxide Research Group, Scripps Institution of Oceanography (SIO), University of California.

Table 9. Molecular masses and mole fractions for dry air currently used (2009) for flow calibrations [32].

Component	**Molecular Mass (g/mol)**	**Mole Fraction (2009)**
Nitrogen	28.01348	0.780854
Oxygen	31.9988	0.209406
Argon	39.948	0.009332
Carbon Dioxide	44.0098	385×10^{-6}
Neon	20.179	18.2×10^{-6}
Helium	4.0026	5.2×10^{-6}
	Average Molecular Mass	28.9653[#]

5.6 Density

Now that the sub-components have been quantified, the uncertainty of density measurements made in the collection tank with nitrogen and argon (for volume determinations and for flow measurements) and with dry air (for flow measurements) can be calculated and they are presented in Tables 10 and 11. For the pure gases, the relative standard uncertainty is 37×10^{-6} and the primary contributor is the pressure measurement. For air, the relative standard uncertainty of the density is 42×10^{-6}. The uncertainties of the density of ambient air (needed for buoyancy corrections) and of distilled water are considered in the section pertaining to tank volume determinations.

Table 10. The uncertainty of collection tank gas density for nitrogen and argon.

Uncertainty Category	**Standard Uncertainty (*k*=1)**		**Contrib**	**Comments**
Collection Tank Density (N_2 & Ar)	**Relative (×10^6)**		**(%)**	
pressure	30	2.99×10^{-3} kPa	64	from Table 5
temperature	20	5.87 mK	28	from Table 7
compressibility	10	1×10^{-5}	7	from Table 8
molecular mass (purity)	1	2.80×10^{-5} g/mol	0	
gas constant	2	1.41×10^{-2} $(cm^2)/(s^2K)$	0	
RSS	**37**	**4.25×10^{-8} g/cm^3**		

Table 11. The uncertainty of collection tank gas density for dry air from the NIST Fluid Metrology Group small compressor and dryer system.

Uncertainty Category	**Standard Uncertainty (*k* =1)**		**Contrib**	**Comments**
Collection Tank Density (Air)	**Relative (×10^6)**		**(%)**	
pressure	30	2.99×10^{-3} kPa	49	from Table 5
temperature	20	5.87 mK	22	from Table 7
compressibility	10	1×10^{-5}	6	from Table 8
molecular mass (purity)	20	5.79×10^{-4} g/mol	24	
gas constant	2	1.41×10^{-2} $(cm^2)/(s^2K)$	0	
RSS	**42**	**2.38×10^{-7} g/cm^3**		

5.7 Collection Time

As explained in section 4.2.3, the collection time is an approximate time measured by timers that is then corrected via analysis of records of the inventory pressure data and trigger voltages to minimize inventory mass and improve uncertainty cancellation. The base time is measured redundantly with two Hewlett-Packard Model 53131A counters.

[#] Constituents with mole fractions below 5×10^{-6} have been omitted. Because mole fractions do not exactly sum to unity ($\sum x_i \neq 1$), the molecular mass has been corrected using $\mathcal{M} = \sum x_i \mathcal{M}_i \Big/ \sum x_i$.

The counter calibration and usage leads to less than 0.01 ms uncertainty. Due to the 3000 Hz recording frequency of the inventory pressure and trigger data, the actual rise of the trigger voltage can be any time within a 0.33 ms window. Assuming a rectangular distribution, the post-processing corrections will have a standard uncertainty of 0.19 ms. This uncertainty applies to both the start and stop times. The time uncertainties of the two pressure measurements used in the mass cancellation procedure are negligible since the times are found by interpolation of the data records and are much smaller than 0.33 ms. The combined collection time uncertainty is 0.3 ms (see Table 12).

Table 12. Collection time uncertainties.

Uncertainty Category	**Standard Uncertainty (k =1)**		**Contrib**	**Comments**
	Relative ($\times 10^6$)	**(ms)**	**(%)**	
Collection Time				
Time value		100000		
timer cal and usage	0	0.01	0	base time uncertainty
inventory correction (start)	2	0.19	50	3000 Hz, rectangular distribution
inventory correction (stop)	2	0.19	50	3000 Hz, rectangular distribution
RSS	**3**	**0.3**		

5.8 Volume of the 34 L and 677 Liter Collection Tanks (Gravimetric Method)

The uncertainty of the determination of the collection tank volume by the previously described gravimetric method (section 4.3.1) is traceable to the uncertainty of the mass and density measurements made during the process, which are in turn dependent on the quantities shown in Fig. 10. The uncertainty of the density measurements for the pure nitrogen and argon gases used for the volume measurements was given in Table 10. The scale used was a Mettler-Toledo model PR10003, which has a 10 kg capacity. The uncertainty of the mass measurements of the high-pressure cylinder before and after discharge is dependent on the buoyancy corrections (ambient air density and cylinder external volume), the reference masses used with the mass comparator, and the performance of the mass comparator. The measurement of the external volume of the

high-pressure cylinder via the Archimedes principle was described in an earlier section. The uncertainty of this measurement is traceable to the density of distilled water, ambient air, reference masses, and the performance of the mass measuring systems.

The uncertainty of the density of ambient air during the course of the various weighing procedures is given in Table 13. The pressure, temperature, and relative humidity uncertainties account for instrument calibration uncertainties as well as variations in the room conditions during the time needed to make a mass measurement. The relative combined uncertainty of the ambient air density is about 500×10^{-6}, with the largest contribution being from temperature.

Table 13. Uncertainty of the density of ambient air.

Uncertainty Category	**Standard Uncertainty (k =1)**		**Contrib**	**Comments**
Ambient air density	**Relative ($\times 10^6$)**		**(%)**	
pressure	129	0.013 kPa	6	cals and change during meas
temperature	336	100 mK	45	cals and change during meas
relative humidity	189394	2.5 %	15	cals and change during meas
equation of state (Z, M, R)	200	0.0002	33	based on literature references
RSS	**513**	**6.02×10^{-7} g/cm^3**		

Table 14. Uncertainty of the external volume of the high-pressure cylinder.

Uncertainty Category	**Standard Uncertainty (k =1)**		**Contrib**	**Comments**
External tank volume	**Relative ($\times 10^6$)**		**(%)**	
apparent mass in air	1	4.61×10^{-3} g	0	
apparent mass in water	-	0.14 g	34	based on water T uncertainties
density of air	513	6.01×10^{-7} g/cm^3	0	correlation and meas unc
density of water	20	2×10^{-5} g/cm^3	15	correlation and meas unc
expansion	20	9.38×10^{-2} cm^3	15	T and P effects
std deviation of repeated meas.	30	0.14 cm^3	35	
RSS	**51**	**0.24 cm^3**		

The uncertainties related to the determination of the external volume of the high-pressure cylinder are listed in Table 14. The 1×10^{-6} relative standard uncertainty for the apparent mass in air is based on uncertainty calculations for the true mass of the weighed cylinder (discussed later). The uncertainty of the apparent mass in water is based on the recorded temperatures of water that made the cylinder barely sink or barely float. Uncertainty of the water temperature for neutral buoyancy of 0.2 K leads to a value for the uncertainty of the apparent mass in water. This uncertainty is not reported in a relative form since the apparent mass in water is zero and the relative uncertainty is therefore undefined. The RSS is calculated using the results in the third column and their sensitivity coefficient. The water density uncertainty includes thermometer uncertainties, estimates of non-uniformity of the water temperature, and uncertainty of the water density correlation obtained from the literature. As previously stated, different values of external volume were used for the full and empty cylinder due to pressure dilation, but an uncertainty related to pressure and temperature effects is included here. The collection tank volume is not very sensitive to this external tank volume, hence larger uncertainty values than $51 \times 10^{-6}\ V_{ext}$ could certainly be tolerated.

Table 15. Uncertainty of the high-pressure cylinder mass measurement.

Uncertainty Category	**Standard Uncertainty (k =1)**		**Contrib**	**Comments**
Final mass of high P cylinder	**Relative ($\times 10^6$)**		**(%)**	
reference masses	0.5	1.91×10^{-3} g	26	from NIST Mass Group cal report
room air density	513	6.01×10^{-7} g/cm^3	45	
reference mass density	0	0 g/cm^3	0	same value for cal. and usage
external cylinder volume	51	0.24 cm^3	1	from unc. of Archimedes method
std deviation of repeated meas.	1	0.002 g	28	
RSS	**1**	**0.00376 g**		

The relative standard uncertainties of the cylinder mass measurement (Table 15) are quite small (1×10^{-6}) with the major components being the reference masses, the room air

density (for buoyancy corrections) and the performance of the comparator (repeatability of the 5 measurements made with the comparator, a type A uncertainty). The complete mass measurement process was repeated several times for the full and empty cylinder conditions to assess the repeatability of the process, and these repeated mass values never differed by more than $1 \times 10^{-6}\ m_c$. This repetition was undertaken since a previously used cylinder showed changes over time, probably due to absorption of water from room humidity variations. The uncertainty of the density of the reference masses (7.8 g/cm^3) is negligible since the sensitivity of mass measurements to this component is extremely small. While some of the mass measurement uncertainties for the full and empty cylinder are correlated and this could be used to reduce the uncertainty of the mass delivered to the collection tank, this benefit was not utilized since the improvement was not significant. A table of uncertainty components of the empty cylinder mass measurement is not presented because it is so similar to Table 15.

Finally, the uncertainty of the collection tank volume is presented in Table 16. The relative value of the initial collection tank density uncertainty is quite large, but the sensitivity of the result to this quantity is very small. Recall that uncertainty due to the effects of room temperature variations on the portion of the collection tank not submerged has already been incorporated as a temperature uncertainty. The effects of pressure changes from vacuum to 100 kPa on the tank volume have been considered analytically and found to be negligible. A small volume (1 cm^3) of connecting tubing and valve was necessary to introduce gas from the pressurized cylinder to the collection tank. This volume was measured with alcohol and a graduated syringe and the uncertainty of this volume correction was estimated to be 0.5 cm^3. By far the largest contribution is from the final gas density, and this in turn is nearly completely traceable to the pressure measurement.

Table 16. Uncertainty of the 677 liter collection tank volume.

Uncertainty Category	**Standard Uncertainty (k =1)**		**Contrib**	**Comments**
Collection tank volume	**Relative ($\times 10^6$)**		**(%)**	
Initial mass of high P cylinder	1	0.00385 g	5	see Table 15
Final mass of high P cylinder	1	0.00376 g	5	see Table 15
initial collection tank gas density	100000	1.14×10^{-9} g/cm^3	0	
final collection tank gas density	37	2.31×10^{-8} g/cm^3	84	see Table 10
expansion due to P and T	0	0 cm^3	0	< 1 ppm
extra volume uncertainty	1	0.50 cm^3	0	related to liq transfer meas.
std deviation of repeated meas.	10	16.78 cm^3	6	8 measurements, 2 gases
RSS	**41**	**27.48 cm^3**		

Each gravimetric volume determination required one day to complete due to the time required to achieve ultimate vacuum in the tank (1 Pa), the time for the pressure transducer to reach thermal equilibrium after filling, and the time to take multiple cylinder mass measurements separated by an hour each time. Eight volume measurements were performed on the 677 L tank, two with UHP nitrogen and six with UHP argon. The average of the eight measurements was 677.936 L and the standard deviation of their mean was $10 \times 10^{-6}\ V_T$. The standard uncertainty for the 677 L volume was reduced from $71 \times 10^{-6}\ V_T$ (2002) to $41 \times 10^{-6}\ V_T$ (2009), primarily due to improvements in the pressure measurements.

As a check, the 2002 measurements of the collection tank volumes were compared to the newer measurements. To do so, the volume of the old and new piping and pressure instrumentation networks was measured while they were separated from the collection tanks. These volume measurements were performed for each piping network using the volume expansion method and a reference volume of 0.53775 L. The volume difference between the two piping networks was 0.0485 L. When this difference was applied, the old and new volume measurements for the 677 L tank agreed within 41 ppm, well within expectations based on the uncertainty analyses.

In 2002 the volume expansion method was used to measure the 34 L collection tank volume. In 2009, the gravimetric method was used, filling the tank twice to increase the mass change in the pressurized cylinder (as explained in section 4.3.1). The uncertainty for the 34 L volume is given in Table 17. Uncertainties due to the initial and final tank gas densities are included twice to account for the double filling.

The average of four measurements of the tank volume was 34.0815 L and the standard deviation of their mean was $10 \times 10^{-6}\ V_T$. Using the difference between the old and new piping networks, the 2009 and 2002 volume measurements for the 34 L tank differed by $29 \times 10^{-6}\ V_T$. The standard uncertainty of the 34 L volume was reduced from $116 \times 10^{-6}\ V_T$ to $58 \times 10^{-6}\ V_T$.

Table 17. Uncertainty of the 34 liter collection tank volume.

Uncertainty Category	**Standard Uncertainty (k =1)**		**Contrib**	**Comments**
Collection tank volume	**Relative ($\times 10^6$)**		**(%)**	
Initial mass of high P cylinder	1	0.00385 g	35	see Table 15
Final mass of high P cylinder	1	0.00376 g	35	see Table 15
initial collection tank gas density (2x)	100000	1.62×10^{-9} g/cm^3	0	
final collection tank gas density (2x)	37	6.00×10^{-8} g/cm^3	20	see Table 10
expansion due to P and T	0	0 cm^3	0	< 1 ppm
extra volume uncertainty	1	0.50 cm^3	6	related to liq transfer meas.
std deviation of repeated meas.	10	0.34 cm^3	3	4 measurements
RSS	**58**	**1.98 cm^3**		

5.9 Leaks

The 34 L *PVTt* standard was designed for use at a minimum flow of 1 L/min, however, the actual lower flow limit is determined by time constraints and by leaks. (This discussion does not distinguish between actual leaks and so-called “virtual leaks” or “out-gassing”.) The 34 L system has been used successfully to calibrate flowmeters at flows

of only 0.01 L/min. Unfortunately, a single flow measurement at this flow takes 28 hours, even if one fills the tank to 50 kPa instead of the normal 100 kPa.

Leaks into the collection and inventory volumes are routinely measured by evacuating them and observing the rate of rise of density over several hours. Typical values from these tests are 1×10^{-6} L/min for the 34 L tank and 8×10^{-6} L/min for the 677 L tank. Because of these leaks, not all of the gas entering the evacuated tank flows through the meter under test: some of it enters from the room or comes from out-gassing of the collection tank walls. In Fig. 11, the leaks are treated as a $k = 1$ uncertainty, a fixed flow uncertainty is root-sum-squared along with the other uncertainty components. (However, in some low flow tests, the leak rate is carefully measured before and after each calibration and included as a correction rather than an uncertainty.) Leaks become significant uncertainty contributors at flows less than 1 L/min for the 677 L standard and less than 0.1 L/min for the 34 L standard.

5.10 Inventory Volume

The mass change in the inventory volume is negligible since we used the mass cancellation procedure. However, since there are imperfections in the procedure, uncertainty components related to the inventory mass change cannot be neglected. Fortunately, the most significant of these uncertainty components (due to sensor time constants) are correlated between the start and stop diversions for the methods of operation used in this flow standard. Other correlated inventory volume uncertainties include the pressure and temperature sensor calibrations and the differences between sensed and stagnation values of pressure and temperature. For instance, the inventory temperature is measured incorrectly low by the same amount at both the start and stop conditions due to slow sensor response time, so cancellation of temperature uncertainty occurs. More precisely, the uncertainty of the mass change within the inventory volume caused by the *correlated* pressure and temperature uncertainties can be expressed as:

$$u(\Delta m_I) = \frac{V_I M}{ZR}\left[\left(\frac{1}{T_I^f}u(P_I^f) - \frac{1}{T_I^i}u(P_I^i)\right)^2 + \left(\frac{P_I^f}{(T_I^f)^2}u(T_I^f) - \frac{P_I^i}{(T_I^i)^2}u(T_I^i)\right)^2\right]^{1/2} \qquad (11)$$

where in this equation, $u(P_I)$, $u(T_I)$, and $u(\Delta m_I)$ are the uncertainties of the inventory pressure, the inventory temperature, and the inventory mass change during the collection, respectively. Note that if the uncertainties and the initial and final conditions are equal (i.e. $u(T_I^i) = u(T_I^f)$, $u(P_I^i) = u(P_I^f)$, $T_I^i = T_I^f$, and $P_I^i = P_I^f$), then the terms within parentheses cancel, and the flow uncertainty related to the inventory volume is zero. Equation 16 demonstrates the benefit of matching the initial and final inventory conditions to optimize the cancellation of correlated uncertainties.

Not all of the measurement uncertainties of the inventory volume are correlated. For perfect inventory mass cancellation, the pressure and temperature measured at specific locations in the inventory volume must exhibit perfect correlation with the pressures and temperatures throughout the inventory volume. In this way, the sensor readings "represent" the conditions throughout the volume and when the readings at the specific locations match, the conditions throughout the inventory volume are matched. Unfortunately, this representative relationship may not exist and there may be inconsistencies between the pressure and temperature fields between the start and stop diversions. These inconsistencies may originate from a change in the inventory wall temperature or from differences in the flow paths between the start and stop diversions. The spatial inconsistencies are uncorrelated and their magnitude is likely a function of the mass flow.

Another source of inventory uncertainty, alluded to previously, is due to imperfection in matching the stop diversion pressure to the start diversion pressure. Recall that the inventory pressure is recorded while the bypass valve is open (nominally the barometric pressure), and that the tank filling is stopped when the inventory pressure regains this same pressure. In this way, the pressure at the beginning of the dead-end time transients is nearly equal for both diversions and the symmetry of the transients is improved. At

high flows, it becomes more difficult to match these initial pressures in the high speed data records and a "trigger pressure difference" that increases with increasing flow occurs. The size of the trigger pressure difference can be reduced by using faster sensors and a fast data acquisition and diverter valve control system. An example of the trigger pressure difference can be seen in Fig. 7, where at times less than zero, the pressure traces differ by about 1.6 kPa. The trigger pressure difference, coupled with the "historical" nature of the inventory pressure measurements due to the sensor time constant, is another reason that matching of the pressure sensor readings does not necessarily lead to matching of the actual conditions in the inventory volume. Hence the trigger pressure difference is another source of inventory uncertainty that scales with the flow.

It is difficult to assess the magnitude of the uncorrelated uncertainties of pressure and temperature between the start and stop diversions in the inventory volume. Our strategy is to estimate the uncorrelated inventory uncertainties and then perform experiments (see Section 7) to confirm that the estimates are reasonable. We assumed that the uncorrelated inventory uncertainties scale with the flow and are essentially zero at the minimum flow of each tank. We will assume values of 3 kPa and 9 K (about 3 % of the nominal values) for the maximum flow of each tank.

Uncertainties related to the fast measurement of pressure with a 700 kPa full scale Heise Model HPO sensor in the inventory volume are listed in Table 18, separated into correlated and uncorrelated components.

The uncertainties of the measurement of temperature in the inventory volume are listed in Table 19, again divided into correlated and uncorrelated components. The uncertainties include calibration, time response, sensed versus stagnation issues, sensor repeatability, and spatial non-uniformity or inconsistency between start and stop diversions.

Table 18. Uncertainties in the inventory pressure measurement, correlated and uncorrelated, for maximum flow conditions.

Uncertainty Category	**Standard Uncertainty (k =1)**		**Contrib**	**Comments**
	Relative ($\times 10^6$)	**(kPa)**	**(%)**	
Inventory Pressure Measurement				
Pressure value		100		
sensor calibration	3000	0.30	0	
sensor time response	1350000	135	100	from inv. model at max flow
sensed vs. stagnation	710	0.071	0	for max flow
RSS (correlated)	**1350004**	**135**		
sensor repeatability	3.00E+02	0.03	0	from calibration data
spatial inconsistency	3.00E+04	3	100	estimated
RSS (uncorrelated)	**30001**	**3.0**		

Table 19. Inventory temperature uncertainties, correlated and uncorrelated, for the maximum flow for each tank.

Uncertainty Category	**Standard Uncertainty (k =1)**		**Contrib**	**Comments**
	Relative ($\times 10^6$)	**(mK)**	**(%)**	
Inventory Thermocouple				
Temperature value		297000		
sensor calibration	337	100	0	
sensor time response	168350	50000	97	from inventory model
sensed vs. stagnation	50	15	0	for max flow
RSS (correlated)	**168351**	**50000**		
sensor repeatability	286	85	0	from calibration data
spatial inconsistency	30303	9000	100	estimated
RSS (uncorrelated)	**30304**	**9000**		

Tables 20 and 21 show the uncertainty in the mass change in the inventory volume for the largest flows in the 34 L and 677 L systems. The relative inventory uncertainty is extremely large since the mass change is nearly zero. The mass change was calculated using the same 3 kPa and 9 K uncorrelated uncertainty values previously discussed. Note that the mass cancellation process leads to weak sensitivity of the inventory mass to the size of the inventory volume. In this analysis we have used large uncertainties, 1000 cm^3 and 50 cm^3 for the 677 L and 34 L systems respectively, yet the contribution from this source is only 1 %. This is fortunate since the size of the inventory volume is often changed depending on the flowmeter under test and this insensitivity means that a nominal inventory volume is acceptable.

Table 20. Uncertainty of the inventory mass change for the 677 L system.

Uncertainty Category	**Standard Uncertainty (k =1)**		**Contrib**	**Comments**
Inventory mass change	**Relative ($\times 10^6$)**		**(%)**	
initial density	42643	6.29×10^{-5} g/cm^3	50	3 kPa and 9 K uncorr. inv. unc.
final density	42643	6.24×10^{-5} g/cm^3	49	3 kPa and 9 K uncorr. inv. unc.
volume	1051800	1000 cm^3	1	see Table 20
RSS	-	**8.48×10^{-2} g**		

Table 21. Uncertainty of the inventory mass change for the 34 L system.

Uncertainty Category	**Standard Uncertainty (k =1)**		**Contrib**	**Comments**
Inventory mass change	**Relative ($\times 10^6$)**		**(%)**	
initial density	42643	6.29×10^{-5} g/cm^3	50	3 kPa and 9 K uncorr. inv. unc.
final density	42643	6.24×10^{-5} g/cm^3	49	3 kPa and 9 K uncorr. inv. unc.
volume	672857	50 cm^3	1	see Table 21
RSS	-	**6.60×10^{-3} g**		

The sub-component uncertainties of gas density, volume, collection time, and inventory mass change above have been combined in Section 5.2 to give the uncertainty in mass flow.

6 Experimental Verification of the Uncertainty of the *PVTt* Flow Standards

Throughout the range 3 L/min to 110 L/min, flows were measured independently using the 34 L and the 677 L collection systems, using a set of critical flow venturis (CFV) as transfer standards, and the two systems agreed within a relative difference of 150×10^{-6}. Double diversions were used to evaluate the 677 L system over a range of 300 L/min to 1600 L/min, and the relative differences between single and double diversions were less than 75×10^{-6}. These differences are within our expectations based on the uncertainty analysis presented in Section 5.

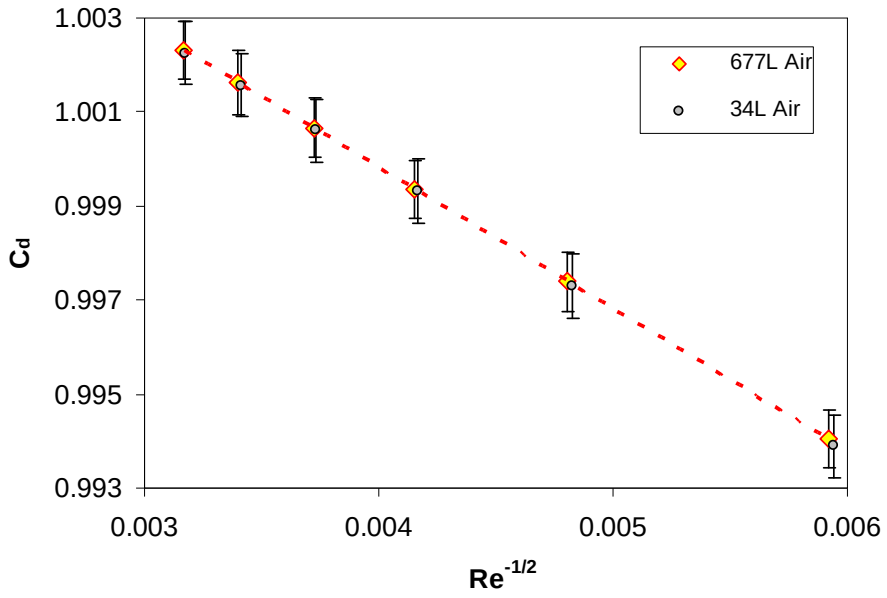

Figure 13. Comparison of the 34 L and 677 L *PVTt* standards using the discharge coefficient of a 1.12 mm nozzle calibrated with air. Each point is the average of six individual flow measurements. Uncertainty bars represent the expanded uncertainty of the C_d measurement.

6.1 Comparison of the 34 L and 677 L Flow Standards

The two flow standards were compared with each other using two critical flow venturis with throat diameters of 1.12 mm and 0.648 mm. The two nozzles were calibrated on both flow standards using six flows of nitrogen and air each. At each flow, three flow measurements were made on two different occasions. A sample of the comparison results for the 1.12 mm nozzle in air is shown in Fig. 13.

The difference between a second order polynomial best fit through the 677 L results and the 34 L results is plotted in Fig. 14, along with results from three other data sets resulting from testing the two nozzles in nitrogen and air. Except for two data points, the results show relative differences between the two standards of $< 80 \times 10^{-6}$. Although there are many correlated uncertainties between the two flow standards, the agreement is well within the propagation of uncertainties analysis and validates the < 0.025 % uncertainty specifications. This is true despite using the 34 L system at flows larger than the 50 L/min crossover flow.

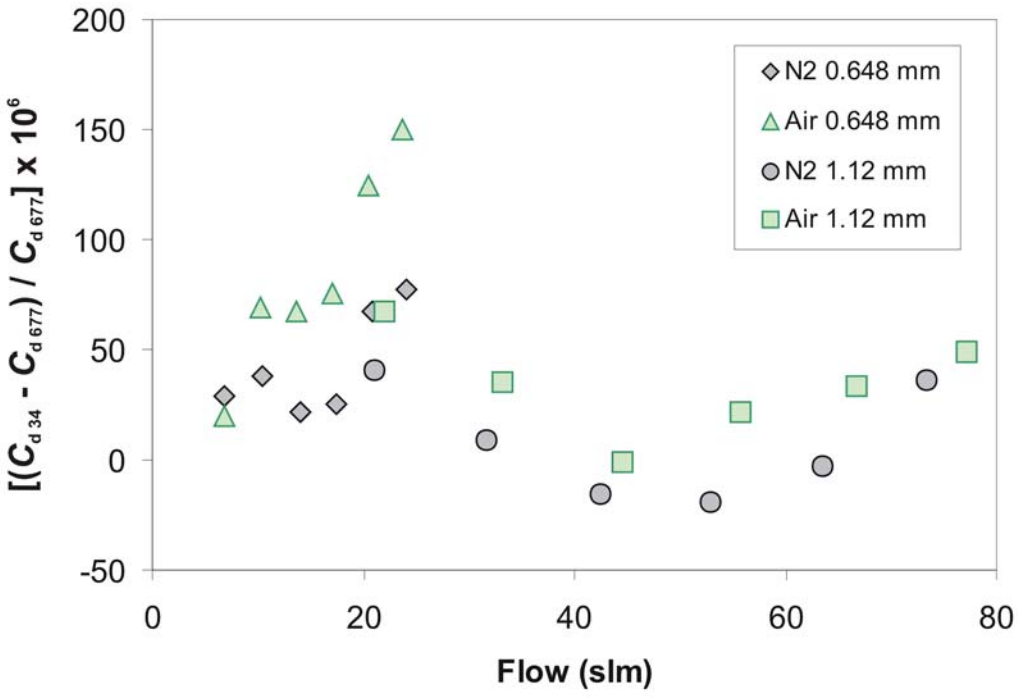

Figure 14. Difference in discharge coefficients measured with the 34 L and 677 L *PVTt* standards for two nozzles calibrated in nitrogen and air.

In another series of experiments, the trigger pressure difference was purposely varied over a range from –2 kPa to 27 kPa at a constant flow of 82 L/min in the 34 L system. The purpose of the test was to measure the dependence of the venturi discharge coefficient on the trigger pressure difference and hence assess its influence on the inventory volume uncertainties. The tests showed a relative change of 10×10^{-6} in discharge coefficient for each 1 kPa change in the trigger pressure difference. Since the largest trigger pressure difference is less than 3 kPa in the present system, this effect is expected to contribute only $30 \times 10^{-6}\ \dot{m}$ to the flow uncertainty. Therefore the major contributor to the inventory uncertainty appears to be spatial inconsistency of the pressure and temperature fields between the start and stop diversions or some other, unknown flow dependent uncertainty source.

6.2 Multiple Diversions in the 677 L Flow Standard

To confirm that the uncertainty analysis for the inventory volume of the 677 L collection system was reasonable, we performed CFV calibrations at identical flows following two different protocols. In the first protocol, the inventory volume was dead-ended at the beginning and end of the collection interval in the usual manner. In the second protocol, the collection interval was divided into two subintervals, i.e. each flow measurement had *two* start and stop diversions. The intermediate dead-end times were set up so that the pressure transients in the inventory volume still permitted the mass cancellation procedure. Breaking the collection into two subintervals has the effect of doubling the uncertainty contribution from the inventory volume. The CFV discharge coefficients from the two protocols were compared to assess the magnitude of the uncertainties introduced by the inventory volume and the flow diversion process. Three flows between 300 L/min and 1600 L/min were tested and the differences in discharge coefficient were all less than $75 \times 10^{-6}\ \dot{m}$ as shown in Table 22.

Table 22. Differences in CFV discharge coefficients (C_d) for two and one diversion in the 677 L flow standard.

Flow (L/min)	**[C_d (2 diversions) – C_d]/C_d × 10^6**
300	53 ± 25
700	-27 ± 31
1600	75 ± 122

7 Summary

We have given a description of the gas flowmeter calibration services that use the 34 L and 677 L *PVTt* primary standards within the NIST Fluid Metrology Group. These *PVTt* standards are used to calibrate flowmeters between 0.01 L/min to 2000 L/min, with uncertainty of 0.025 % or less. For reasons of time efficiency, the normal crossover flow between the two standards is 50 L/min. However, if the crossover flow is moved to 10 L/min and the flow range is restricted to 0.1 L/min to 1000 L/min, the uncertainty is only 150 ppm. Comparisons of the two calibration standards support this uncertainty specification (see Fig. 14).

The intended audience for this document is potential flowmeter calibration customers, hence we have attempted to address their likely questions. We have described the method of operation of the primary standard and have given the uncertainty analysis for a mass flow measurement (see Tables 2 and 3). We have given a description of the standard gas flow calibration, including a sample calibration report, as well as sources for instructions for submitting a flowmeter for calibration.

The 34 L and 677 L *PVTt* flow standards have several novel features. The collection tanks are immersed in a water bath that matches the nominal room temperature and is stable and uniform to 1 mK. The collection tanks are divided into sections of small enough diameter that the gas inside them achieves thermal equilibrium with the surrounding water bath in 20 minutes or less. This reduces the contribution of temperature to the flow measurement uncertainty to a low level.

Uncertainties related to the inventory volume and the diversion of gas into the collection tank at the start and stop of a flow measurement have been studied in great detail. A thermodynamic model of the inventory volume during diversion has been utilized to understand the large pressure and temperature transients and the importance of sensor time constants on the flow measurement uncertainty. The flow standard is operated to achieve "mass cancellation" in the inventory volume, thereby taking advantage of correlated sensor uncertainties to minimize uncertainty contributions from the inventory volume. The uncertainty contributions of the inventory volume have been considered from both the time and mass perspectives. The volumes of the collection tanks were measured by the gas gravimetric method with standard uncertainty $< 58 \times 10^{-6}\ V_T$.

A detailed uncertainty analysis for the gas flow standard shows that the 677 L system measures mass flow with an uncertainty between $126 \times 10^{-6}\ \dot{m}$ and $254 \times 10^{-6}\ \dot{m}$ ($k = 2$). The higher uncertainty applies to higher flows as the inventory transients and the related uncertainties grow larger. For the 34 L tank, the uncertainties range from $151 \times 10^{-6}\ \dot{m}$ to $228 \times 10^{-6}\ \dot{m}$ ($k = 2$). For pure gas measurements, the largest sources of uncertainty can be traced to pressure measurement (about $60 \times 10^{-6}\ P$, $k = 2$) which is the major contributor to gas density and tank volume uncertainties.

Comparisons between the 34 L and 677 L standards from 3 L/min to 100 L/min show agreement within $150 \times 10^{-6}\ \dot{m}$ or better. Experiments using single diversions (normal operation) and double diversions to the collection tank were used to validate the uncertainty estimates of the 677 L inventory volume and the differences between these two methods were less than $75 \times 10^{-6}\ \dot{m}$. The evaluation results, comparisons to previously existing gas flow standards, and an international key comparison [34] support the uncertainty statements for the 34 L and 677 L *PVTt* standards.

[34] Wright, J. D., Mikan, B., Paton, R., Park, K.-A., Nakao, S.-I., Chahine, K., Arias, R., *CIPM Key Comparison for Low-Pressure Gas Flow: CCM.FF-K6*, Metrologia, **44,** 2007**.**

National Institute of Standards and Technology
Technology Administration, U.S. Department of Commerce

Appendix: Sample Calibration Report

REPORT OF CALIBRATION

FOR

A CRITICAL FLOW NOZZLE

December 1, 2009

Mfg.: Meter Builders, Inc.
Serial No: 1234
Throat Diameter: 0.125 in (0.3175 cm)

submitted by

Flowmasters, Inc.
Metertown, MD

Purchase Order No. A123 dated June 23, 2003

The flow meter identified above was calibrated by flowing filtered dry air through it into a volumetric prover (the NIST 677 L *PVTt* standard). The *PVTt* standard determines mass flow, $\dot{m}$, by measuring the change in density of gas diverted into a known volume for a measured period of time.[1] The flow meter was tested at six flows; three (or more) measurements were gathered at each flow on two different occasions and used to produce averages at each flow.

A photograph of the flow meter installation is shown in Figure 1. The nozzle temperature, (T_1), and pressure, (P_1), were measured with NIST sensors, (Hart Scientific Chub-E4 SN A27253, thermistor #3, and Hirai SN MD11A001). Stagnation temperature, T_0, was calculated from the measured temperature via the following equation, using a recovery factor, r, of 0.75:

$$T_0 = T_1 \cdot \left[1 + \frac{\gamma - 1}{2} \cdot M^2 \cdot (1 - r) \right] \qquad (1)$$

and the stagnation pressure, P_0, was calculated via the equation:

[1] Wright, J. D., Johnson, A. N., Moldover, M. R., and Kline, G. M., *Gas Flowmeter Calibrations with the 34 L and 677 L PVTt Standards*, NIST Special Publication 250-63, December 4, 2009.

$$P_0 = P_1 \cdot \left[1 + \frac{\gamma - 1}{2} \cdot M^2 \right]^{\frac{\gamma}{\gamma - 1}} \qquad (2)$$

where γ is the specific heat ratio and M is the Mach number in the approach pipe (with diameter = 2.21 cm), both based on P_1 and T_1.[2] The largest of these corrections is 0.043 % for pressure.

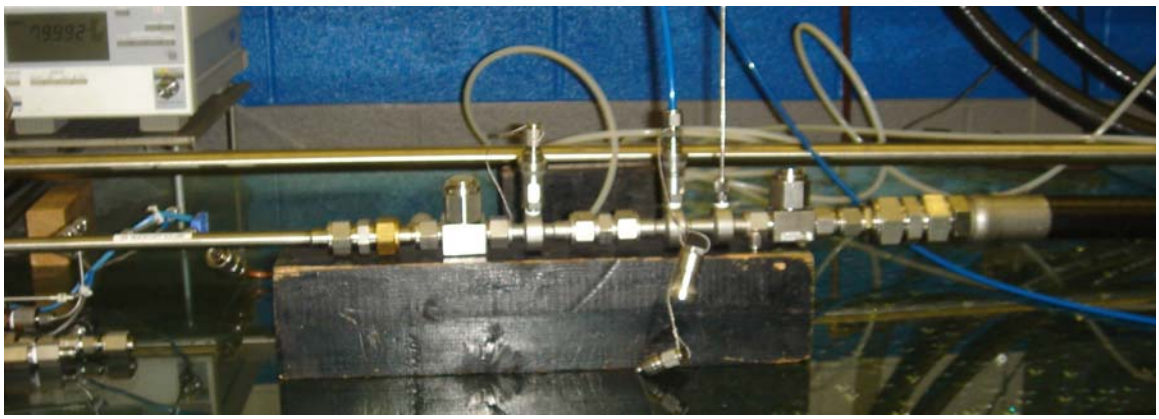

Figure 1. Photograph of the flow meter installation.

The Reynolds number is included in the tabulated data and it was calculated using the following expression:

$$Re = \frac{4 \cdot \dot{m}}{\pi \cdot d \cdot \mu} \qquad (3)$$

where $\dot{m}$ is the mass flow of gas, d is the nominal nozzle throat diameter, and μ is the gas viscosity, all in consistent units so that Re is dimensionless. The gas properties (density and viscosity) were calculated using the NIST gas properties database.[3]

The discharge coefficient C_d was calculated from the expression:

$$C_d = \frac{4 \cdot \dot{m} \cdot \sqrt{R \cdot T_0}}{\pi \cdot d^2 \cdot P_0 \cdot C^*} \qquad (4)$$

where R is the gas constant [the universal gas constant, 8.314471 J / (mol K), divided by the gas molecular mass, 28.9653 g/mol for air. The real critical flow factor, C^*, was also calculated from the NIST gas properties database.

---

[2] *Measurement of Gas Flow by Means of Critical Flow Venturi Nozzles*, ISO 9300: 1990 (E), International Organization for Standardization, Geneva, Switzerland, 1990.

[3] Lemmon, E. W., McLinden, M. O., and Huber, M. L., Refprop 23: Reference Fluid Thermodynamic and Transport Properties, NIST Standard Reference Database 23, Version 8.1, National Institute of Standards and Technology, Boulder, Colorado, 2007.

The calibration results are presented in the following table and figure. The figure shows the discharge coefficient as a function of the inverse square-root of the Reynolds number. For many ISO standardized nozzles in the laminar flow range[4] this has the effect of linearizing the calibration data.

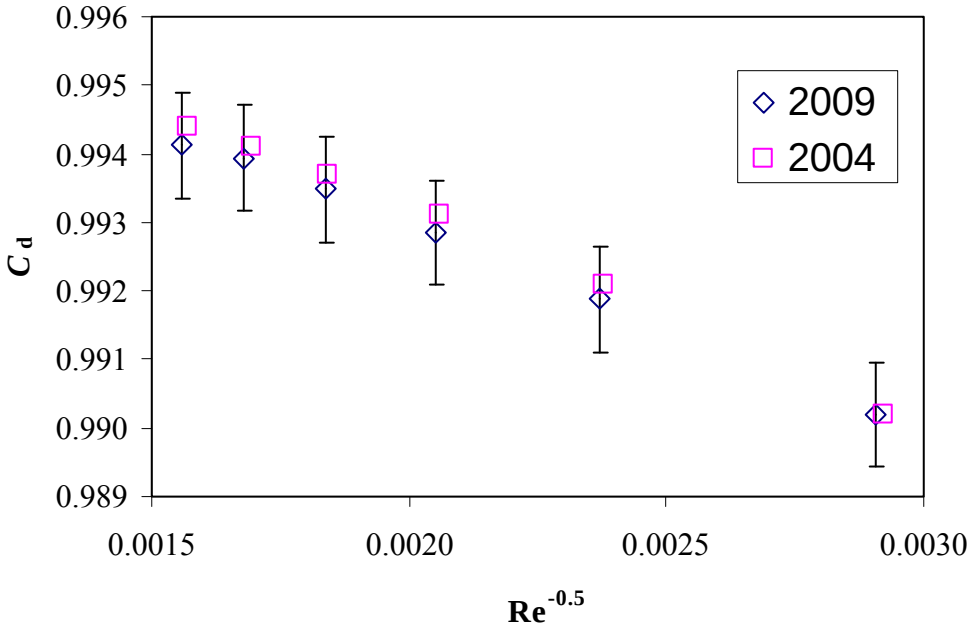

Figure 2. Calibration results for 0.180 inch (0.4572 cm), SN 1234 nozzle tested using air.

An analysis was performed to assess the uncertainty of the results obtained for the meter under test.[5, 6, 7] The process involves identifying the equations used in calculating the calibration result (measurand) so that the sensitivity of the result to uncertainties in the input quantities can be evaluated. The approximately 67 % confidence level uncertainty of each of the input quantities is determined, weighted by its sensitivity, and combined with the other uncertainty components by root-sum-square to arrive at a combined uncertainty (U_c). The combined uncertainty is multiplied by a coverage factor of 2.0 to arrive at an expanded uncertainty (U_e) of the measurand with approximately 95 % confidence level.

---

[4] *Measurement of Gas Flow by Means of Critical Flow Venturi Nozzles*, ISO 9300: (E), International Organization for Standardization, Geneva, Switzerland, 1990.

[5] International Organization for Standardization, *Guide to the Expression of Uncertainty in Measurement*, Switzerland, 1996 edition.

[6] Taylor, B. N. and Kuyatt, C. E., *Guidelines for Evaluating and Expressing the Uncertainty of NIST Measurement Results*, NIST TN 1297, 1994 edition.

[7] Coleman, H. W. and Steele, W. G., *Experimentation and Uncertainty Analysis for Engineers*, John Wiley and Sons, 2nd ed., 1999.

Table 1. Calibration results for 0.180 inch (0.4572 cm), SN 1234 nozzle tested using air.

P_0 [kPa]	T_0 [K]	$\dot{m}$ [g/s]	T_{DP} [K]	C^* [-]	Re [-]	C_d [-]	U_e [%]
201.91	292.98	7.75725	257.22	0.6854	118347.26	0.9904	0.06
302.84	292.70	11.66580	257.28	0.6857	177959.57	0.9921	0.06
403.56	292.72	15.56725	257.56	0.6860	237254.11	0.9932	0.06
503.86	292.85	19.45350	257.60	0.6863	296120.94	0.9938	0.06
603.01	292.93	23.29951	257.51	0.6866	354286.04	0.9943	0.06
702.39	293.18	27.14513	257.58	0.6868	412128.49	0.9946	0.06

As described in the references, if one considers a generic basis equation for the measurement process, which has an output, y, based on N input quantities, x_i,

$$y = y(x_1, x_2, \ldots, x_N) \tag{5}$$

and all uncertainty components are uncorrelated, the normalized expanded uncertainty is given by,

$$\frac{U_e(y)}{y} = k\frac{U_c(y)}{y} = k\sqrt{\sum_{i=1}^{N} s_i^2 \left(\frac{u(x_i)}{x_i}\right)^2} \tag{6}$$

In the normalized expanded uncertainty equation, the $u(x_i)'s$ are the standard uncertainties of each input, and s_i' s are their associated sensitivity coefficients, given by,

$$s_i = \frac{\partial y}{\partial x_i}\frac{x_i}{y} \tag{7}$$

The normalized expanded uncertainty equation is convenient since it permits the usage of relative uncertainties (in fractional or percentage forms) and of dimensionless sensitivity coefficients. The dimensionless sensitivity coefficients can often be obtained by inspection since for a linear function they have a magnitude of unity.

For this calibration, the uncertainty of the discharge coefficient has components due to the measurement of the mass flow by the primary standard, $u(\dot{m}) = 0.0125$ %,[8] as well as

[8] Wright, J. D. and Johnson, A. N., *Lower Uncertainty (0.015 % to 0.025 %) of NIST's Standards for Gas Flow from 0.01 to 2000 Standard Liters / Minute*, Proc. of the 2009 Measurement Science Conference, Anaheim, CA, 2009.

the pressure, $u(P) = 0.02\,\%$, and temperature, $u(T) = 0.03\,\%$, measurements at the meters under test. The sensitivity coefficients for mass flow and pressure are 1, and the sensitivity coefficient for temperature is ½. This uncertainty analysis assumes that the user will use the same values for the throat diameter and the critical flow factor given herein and that the uncertainties in these quantities are correlated and cancel.

The present uncertainty analysis does not include uncertainty in the experimental measurements of viscosity found in the references, which can amount to 1 % or more. To prevent errors due to viscosity, the user must use the same gas and viscosity expression used by NIST when using the results given in Table 1, or must use calibration coefficients calculated with their preferred viscosity relationship. Flow measurements made with this nozzle and a gas other than air (including humid air) will have greater uncertainty than that given in the present analysis due to uncertainty in the gas viscosity. Given these assumptions, the viscosity uncertainty depends primarily on the uncertainty of the gas temperature measurement.

To measure the reproducibility[9] of the test, the standard deviation of the discharge coefficient at each of the nominal flows was used to calculate the relative standard uncertainty (the standard deviation divided by the mean and expressed as a percentage). The reproducibility was root-sum-squared along with the other uncertainty components to calculate the combined uncertainty. Using the values given above results in the expanded uncertainties listed in the data table and shown as error bars in the figure.

For the Director,
National Institute of Standards and Technology

Dr. John D. Wright
Project Leader, Fluid Metrology Group
Process Measurements Division
Chemical Science and Technology Laboratories

Ms. Gina M. Kline
Physical Science Technician, Fluid Metrology Group
Process Measurements Division
Chemical Science and Technology Laboratories

[9] Reproducibility is herein defined as the closeness of agreement between measurements with the flow changed and then returned to the same nominal value.